ANALYSIS AND SIMULATION OF A SUBMARINE STEERING CONTROL SYSTEM

Ernest Everett Wessman

NAVAL POSTGRADUATE SCHOOL
Monterey, California

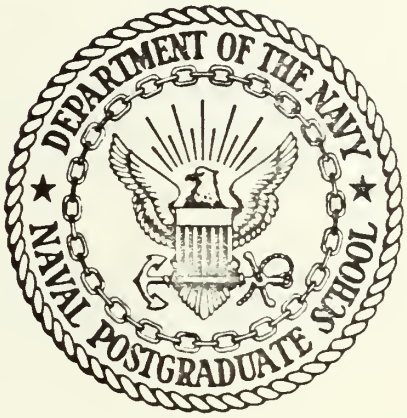

THESIS

Analysis and Simulation
of a
Submarine Steering Control System

by

Ernest Everett Wessman

Thesis Advisor: R. H. Nunn

June 1972

Analysis and Simulation
of a
Submarine Steering Control System

by

Ernest Everett Wessman
Ensign, United States Navy
B.S., M.E., University of Utah, 1971

Submitted in partial fulfillment of the
requirements for the degree of

MASTER OF SCIENCE IN MECHANICAL ENGINEERING

from the

NAVAL POSTGRADUATE SCHOOL
June 1972

ABSTRACT

An existing computer simulation of a hydraulic submarine steering control system was analyzed to determine the source of its unrealistic behavior, which included verifying mathematical equations and numerical parameters, duplicating the simulation on another computer, and investigating the validity of the assumptions made in its development. Rudder turning rate and load pressure drop oscillations which were thought to be unrealistic were caused by the neglect of significant rudder moments related to the control surface turning rate. Knowledge of actual system performance was found to be incomplete and further research was suggested. Potentially beneficial modifications in the servovalve and actuator simulators were identified. Continuing work in the field of unsteady rudder behavior was suggested in order to improve simulator and actual system designs.

TABLE OF CONTENTS

LIST OF TABLES

LIST OF DRAWINGS

LIST OF SYMBOLS

A	actuator piston area
A_{CH}	crosshead area
A_p	area of an incremental flat plate used in the calculation of stationary rudder damping
A'	area of holes in crosshead
C	loss coefficient of a short tube orifice. Also the chord length of a rudder.
c	radial clearance of a crosshead in its sleeve
C_D	coefficient of friction of the stock bearing
C_{MH}	dimensionless twisting moment coefficient
C_{MHO}	quasi-stationary portion of C_{MH}
D	diameter of axial holes in crosshead
db	dead band, fraction of maximum
e	eccentricity of crosshead in sleeve. Also the error signal.
I	polar moment of inertia of the rudder
K_1	amplifier gain coefficient
K_2	flapper centering spring rate
K_3	wand spring rate
K_4	pilot stage valve flow coefficient
K_5	main stage valve flow coefficient
K_6	system hydraulic resilience coefficient
K_7	hydrodynamic load torque coefficient
K_8	hydrodynamic load torque coefficient
K_9	lift coefficient
K_{10}	seal friction coefficient
K_{11}	drag coefficient

K_{12}	mechanical resilience coefficient
L	tiller length
l	length of various holes or channels
M	number of holes in crosshead, and also symbol for moment
M_H	twisting moment generated by a rotating rudder in a moving fluid
N	number of slots in the crosshead
P_1	pressure in the forward, enclosed portion of the crosshead sleeve
P_2	pressure in the aft, open portion of the crosshead sleeve
P_L	load pressure drop
P_{Lmax}, P_{Lm}	maximum load pressure drop
P_S	supply pressure
$\dot{P}_L$	rate of change of the load pressure drop
Q	hydraulic fluid flow rate
Q_C	flow rate through an annulus formed between two eccentric cylinders
Q_S	flow through the rectangular slots
Q_O	flow through the crosshead holes
R	rudder stock radius
r	radius of the crosshead sleeve. Also distance from the pivot line of the rudder.
S	rudder span
T_{CH}	equivalent torque generated by the crosshead
T_F	friction torque
T_H	hydrodynamic torque
T_{Hmax}, T_{Hm}	maximum hydrodynamic torque
T_P	pressure torque
$T_{\dot{\theta}}$	rudder torque generated by a rotating rudder immersed in a stagnant fluid

T_S	system sliding friction torque
U	velocity of the fluid past the rudder
V	ship velocity
V_O	maximum ship velocity
W	weight of rudder
w	width of rectangular slot
x	valve flapper displacement
y	hydraulic actuator displacement
$\dot{y}$	hydraulic actuator velocity
y_{max}, y_m	maximum hydraulic actuator displacement
$\dot{y}_m$	maximum actuator velocity
z	valve spool displacement
$\dot{z}$	valve spool velocity
z'	effective valve spool displacement after compensation for spool dead zone effects
z''	effective valve spool displacement after compensation for spool dead zone and multiple flow gain effects
α	rudder angle of attack to oncoming stream
β	time scaling factor for analog program
ΔC_{MH}	rudder turning rate - dependent portion of C_{MH}
ΔM_H	rudder turning rate - dependent portion of the rudder twisting moment
ν	kinematic viscosity
μ	absolute viscosity
Ω	$\frac{\alpha U}{c\frac{d\alpha}{dt}}$
θ	rudder angle
θ_{max}, θ_m	maximum rudder angle
$\dot{\theta}$	rudder angular velocity

ACKNOWLEDGEMENT

The writer wishes to thank his thesis advisor, Associate Professor R. H. Nunn of the Naval Postgraduate School's Mechanical Engineering Department for his patience and assistance. He also wishes to acknowledge the contributions of the following:

Mr. Guy Johnson, Naval Ship Research and Development Center

Mr. Walter Blumberg, Naval Ship Research and Development Center

Mr. Ralph Leibowitz, Naval Ship Research and Development Center

Mr. Leeland Smith, Mare Island Naval Shipyard

Mr. William Kendall, Mare Island Naval Shipyard

Professor George Thaler, Naval Postgraduate School

Mr. Robert Limes, Naval Postgraduate School

I. THE NATURE OF THE PROBLEM

A. BACKGROUND INFORMATION

In 1971, the Naval Ship Research and Development Center (NSRDC), in Annapolis, Maryland, identified a potential stability problem in an electrohydraulic servosystem which was being developed. The control system was being designed to control the movement of a submarine's rudder in accordance with commands from the helmsman. The NSRDC developed an analog computer simulation (hereafter referred to as the "baseline simulation") which incorporated many of the characteristics of an actual hydraulic control system, including friction, hydraulic and mechanical characteristics, servovalve behavior, and interdependence of elements necessary to create a simulation of the actual system. The simulation was based on equations developed to model an existing system used in the USS PARGO (SSN 650). Provisions were made so that the simulation could be adjusted by changing values of the various components of the model, in order to conform to possible changes of the parameters of the system under development, such as changes in dimensions, materials, and operating conditions. The provision for adjustment of the simulator parameters also allowed simulation of other existing hydraulic systems of this type. All parameters which were assumed to be of significant impact on the performance of the system were incorporated into the simulation.

When the simulator parameters were arranged to model the performance of the system under development, the model did not conform to expected system behavior; oscillations in pressures and control surface turning

rates were observed which had not been observed in similar systems in use. Further investigations failed to reveal any obvious errors in the simulation, or deficiencies in the parameters which were believed to be of significant impact on the performance of the system.

This thesis is a result of a project initiated in support of the simulation attempt at the NSRDC. The purpose of this project was to determine the reasons for the observed behavior of the hydraulic system model, and to develop appropriate modifications and refinements of the baseline simulation, in order to more closely model actual system performance.

B. SYSTEM UNDER STUDY

1. Introduction

The following paragraphs describe the general characteristics of the idealized system that the NSRDC used in the development of its simulation. The description does not completely describe any real system. Rather, it is a model which was designed to include all of the steering system characteristics that were expected to be of significant impact on the performance of the system.

2. General System Descriptions

The steering system (Figure 1) included the servovalve, connecting tubing, actuating ram, mechanical linkages, rudder, and minor components. The operation of the system is described below. (Numbers in parentheses refer to corresponding labeled parts on Figure 1.)

A desired change of rudder angle is initiated by moving the control wheel (1) by hand, which generates an electrical signal having a voltage proportional to the degree of movement. This voltage representing the desired control surface angle is then compared with a voltage proportional

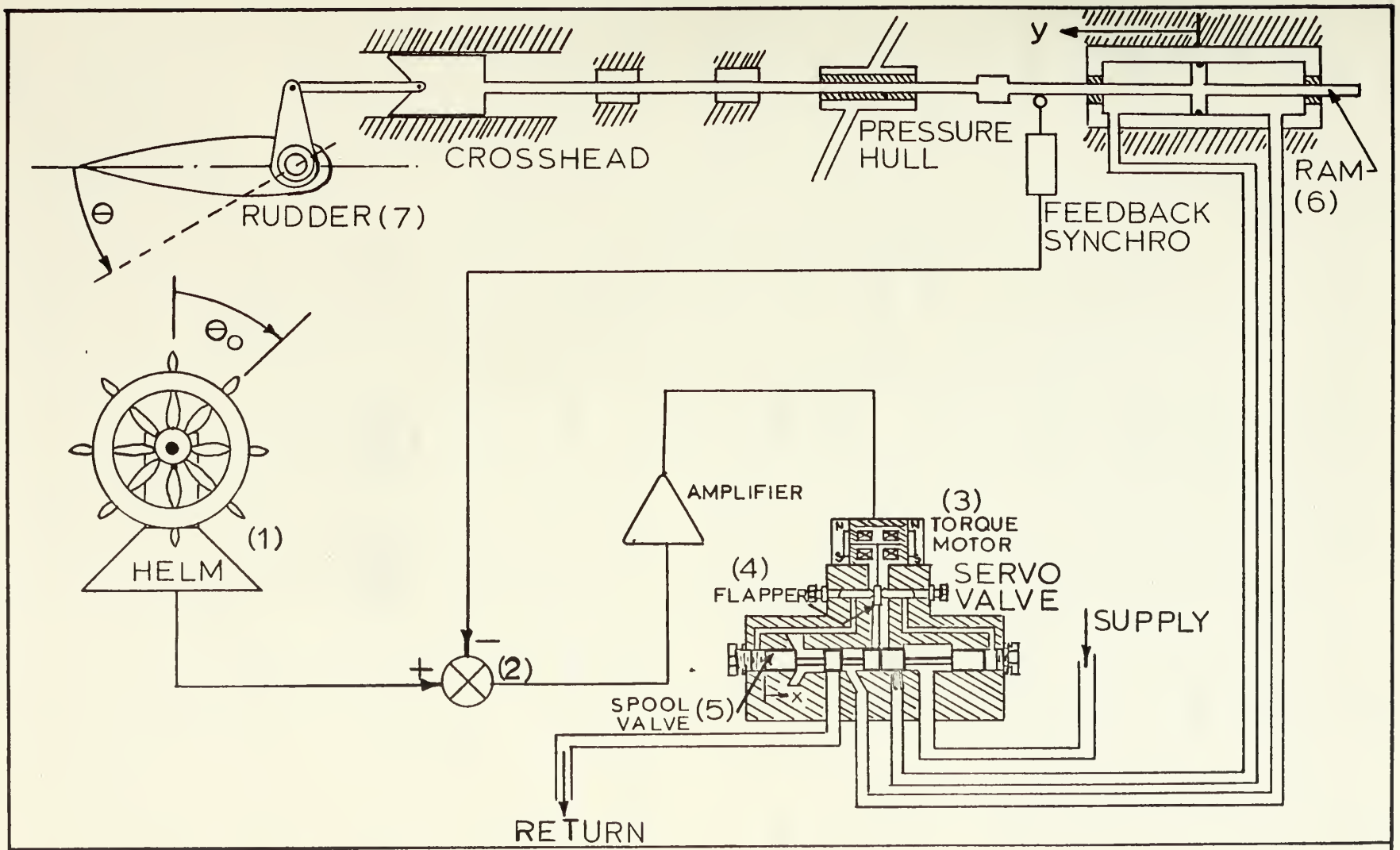

FIGURE 1
SUBMARINE STEERING CONTROL SYSTEM

to the actual position of the hydraulic ram (6). An error signal is generated which approximates the difference between the desired and actual rudder positions (2). This signal actuates an electric torque motor (3) in the servovalve, which moves a small flapper (4) located in the narrow space between two nozzles, causing an increase in the pilot pressure on one nozzle, and a decrease on the other. This difference in pressure causes the spool valve (5) to move, thereby permitting pressure and subsequent fluid flow to be applied to the hydraulic ram (6), resulting in a correcting movement of the control surface (7) through the mechanical linkage. The value of the error signal is modified by movement of the hydraulic ram, and the entire process is continuously repeated until the error signal is reduced to zero. As the error signal decreases, the servovalve closes, control surface movement ceases, and equilibrium is established at the new position.

a. Component Descriptions

(1) Servovalve. The servovalve (Figure 2) used in a submarine steering control system is a two-stage, force feedback model, incorporating a torque motor actuated by an electrical error signal; a flapper-type pilot valve, the flapper itself also serving as the armature of the torque motor; and a spool valve, actuated by the fluid flow caused by the movement of the pilot flapper valve. Movement of the spool results in the direction of fluid flow to the actuating ram.

(2) Actuator. The actuator is a linear, two-way hydraulic ram. The NSRDC assumed in modeling the actuator that it was of compensated construction; that is, it was designed with equal effective areas on both sides of the piston. O-rings are incorporated into the design of the actuator, eliminating essentially all leakage from one side of the piston to the other.

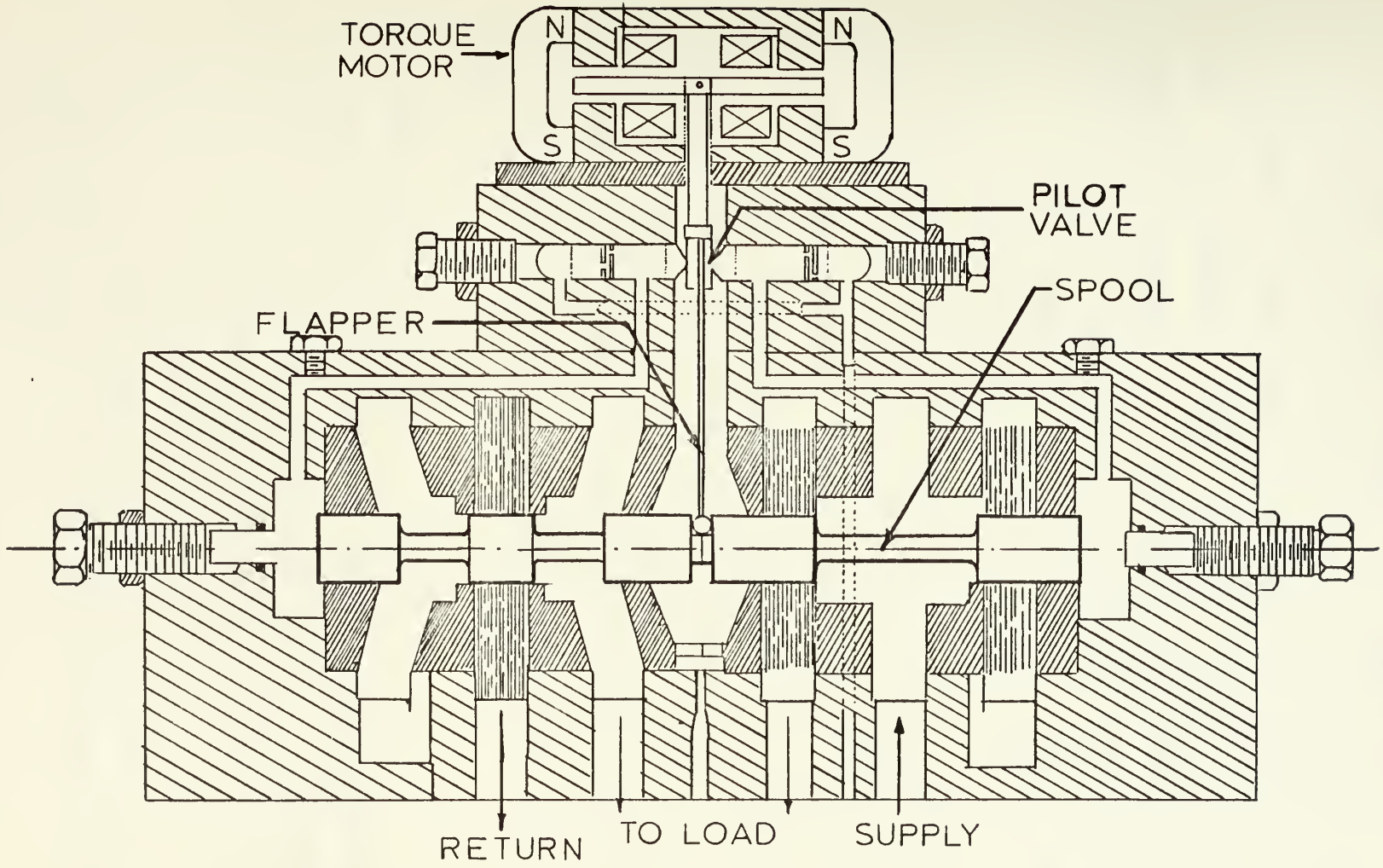

FIGURE 2
SERVOVALVE

(3) Mechanical Linkage. The linkage connecting the hydraulic ram to the rudder consists of a long shaft, support bearings, a packing at the penetration of the pressure hull, a crosshead at the end of the shaft opposite the ram, and a rod connecting the crosshead to the rudder tiller. The crosshead provides a supported, pinned joint from which the connecting rod originates. It was assumed to be constrained from lateral movement by an open-ended sleeve which was flooded with sea water.

(4) Rudder. The rudder is composed of two portions, an upper rudder and a lower rudder, interconnected to the tiller by a single shaft, and located on the top and bottom of the ship's hull, respectively. The rudder is symmetric along the chord length, and is designed for operation within the range of left 35 degrees rudder to right 35 degrees.

(5) Other Components. Other components include piping; an electric transmitter associated with the control wheel; an error feedback servo associated with the actuator; a hydraulic pressure supply which is assumed for design purposes to be constant in pressure, and not subject to influence by steering system conditions; and a petroleum-base hydraulic fluid.

C. NSRDC BASELINE SIMULATION

The following sections describe the work done at the NSRDC in order to simulate the submarine steering control system. The governing equations for each of the components are stated as they were derived by the NSRDC, along with any assumptions that were explicitly stated. A schematic circuit diagram of the analog computer arrangement is presented, and comments from the NSRDC about the nature of the problem and suspected origins of the oscillation are stated.

1. Governing Equations and Assumptions

The governing equations that were provided for each of the components are listed verbatim in this section. Only the governing equations, assumptions, and values for constants were communicated to the writer. Consequently, the procedure by which the expressions were derived, whether through experimentation, experience-justified simplification of complicated transfer functions, or some other way, is unknown. See Appendix A for explanations of the notation used.

a. Servo Valve

The servo valve equations include expressions for the valve flapper displacement, spool valve displacement, nonlinearity compensations, and fluid flow rates through the valve.

(1) Valve Flapper Displacement. The valve flapper displacement, x, is expressed as

$$x = \text{sat}\left[\frac{1}{K_2}(K_1(\theta_o-\theta)-K_3 z)\right]_{-.003}^{+.003} \tag{1}$$

where K_1 is the amplifier gain coefficient, K_2 is the flapper centering spring rate, θ_o is the desired position of the rudder, θ is the actual position of the rudder, K_3 is the wand spring rate, and z is the present valve spool position. No explicit assumptions were given with regard to this equation.

(2) Valve Spool Displacement. The valve spool displacement is obtained through the variation with time of the valve spool velocity $\dot{z}$:

$$\dot{z} = \begin{cases} 0.5 & z \geq .5 \text{ and } SGN(z) = SGN(x) \\ K_4 x & \text{otherwise} \end{cases} \tag{2}$$

where K_4 is the pilot-stage valve flow coefficient. This expression is

best explained by stating that the spool velocity is proportional to the flapper valve displacement, until the spool is fully displaced against the valve body, where the movement must of course cease. The velocity again becomes non-zero only if the direction of movement is reversed, and the valve is allowed to travel away from the hard restraining block.

Nonlinear effects in the valve, such as varying flow gain (i.e., flow is not proportional to spool displacement, due to the shape of the ports used in the spool valve), spool friction, deadband, and torque motor hysteresis are included in the next equations.

Dead band is included in the system through the implementation of the following equations:

$$z' = \begin{cases} z - db & \text{where} \quad z > db, \; z > 0 \\ z + db & \text{where} \quad |z| > db, \; z < 0 \\ 0 & \text{if} \quad -db < z < db \end{cases} \tag{3}$$

where z' is the valve spool displacement after adjustment for spool dead zone. These expressions give the effective spool displacement, i.e., adjust the spool displacement to the value it would have for the given flow if no dead zone were constructed in the valve.

Multiple flow gain is accommodated by combining z' with $z'|z'|$:

$$z'' = .5z' + .5z'|z'| \; . \tag{4}$$

where z'' is the valve spool displacement after spool dead zone, and after multiple flow gain.

Compensation for other nonlinearities such as spool friction and torque motor hysteresis may have been accomplished through adjustment of the coefficients in the equations for spool dead band, and

multiple flow gain. No additional expressions for these nonlinearities were given.

(3) Flow Equation. The flow rate in the spool is related to the corrected spool displacement z", the load pressure drop P_L, and the supply pressure P_s by the following expression:

$$Q = z''K_5 \text{sgn}(P_s - \text{sgn}(z)P_L)\sqrt{P_s - \text{sgn}(z)P_L} \qquad (5)$$

where K_5 is the main-stage valve flow coefficient. No explicit assumptions were listed for this equation.

b. Actuating Ram

The position of the actuating ram is described in two ways; by the position of the rudder itself, and by the integral of the flow rate which has passed through the valve.

(1) Ram Position in Terms of Rudder Position. The ram position y is related to the rudder position, with correction for mechanical resilience in the linkage, by

$$y = L\sin\theta + \frac{AP_L}{K_{12}} . \qquad (6)$$

where L is the length of the tiller, θ is the rudder angle in degrees, K_{12} is the mechanical resilience coefficient of the system, and A is the actuator piston area.

(2) Ram Velocity Expressed in Terms of Pressure Change and Flow. The NSRDC determined that the ram velocity, flow rate, and load pressure have the following relationship to one another:

$$Q = -A\dot{y} + K_6\dot{P}_L \qquad (7)$$

where K_6 is the system hydraulic resiliance, and $\dot{P}_L$ is the rate of change of load pressure drop.

In the development of these equations it was assumed that there was no leakage from the control valve to the actuating cylinder at line connections, seals, and so forth, and that there was no internal leakage in the actuating cylinder itself. Also, it was assumed that a compensated actuator was used; that is, an actuator was used in which both areas, on opposite sides of the piston, were equal.

c. Forces and Torques on the System

All forces on the system were expressed in terms of the equivalent torques which were placed on the rudder structure. A moment balance can then be written:

$$I\ddot{\theta} = Tp + T_H + T_F \qquad (8)$$

where I is the polar moment of inertia of the rudder mass and the included water mass, $\ddot{\theta}$ is the angular acceleration of the rudder, T_p is the torque developed as a result of the pressure drop across the actuator, T_H is the hydrodynamic torque, and T_F is the friction torque. Each torque will now be discussed in more detail.

(1) Friction Torque. T_F is the most complicated of the torques to describe. It is the combined friction torques from the shaft seals, the resultant of the normal force on the rudder bearing surface, and any other sources of sliding (coulomb) friction present in the system. Stationary objects in contact with each other stick together until subjected to forces larger than the friction force present between the objects. Additionally, the level of applied force necessary to sustain movement at very low speeds usually exceeds the force needed at higher velocities. In order to model these system characteristics, the NSRDC developed the following expressions for T_F:

$$T_F = \begin{cases} -(T_H+T_p) & \text{if } |T_H+T_p| < T_S \\ -T_S \text{sgn}(T_H+T_p) & \text{if } |T_H+T_p| > T_S \end{cases} \quad \dot{\theta} < \varepsilon$$

$$-T_C \text{sgn}(\dot{\theta}) \qquad |\dot{\theta}| > \varepsilon \tag{9}$$

where ε is theoretically zero, but in practice is set to approximately 0.2 percent of the maximum angular velocity of the rudder. $T_C = kT_S$, where k is slightly less than one, typically 0.95, and T_S is expressed by

$$T_S = C_D R \left[W + \sqrt{(K_9\theta)^2 + K_{11}\theta + A \cdot P_L)^2} \right] + K_{10} \tag{10}$$

where C_D is the coefficient of friction of the stock bearing, W is the weight of the rudder, R is the rudder stock radius, K_9 is the lift coefficient of the rudder, K_{11} is the drag coefficient of the rudder, and K_{10} is the seal friction coefficient. It should be noted that the NSRDC equation for friction torque did not include any terms for damping proportional to angular velocity of the rudder surface.

(2) Hydrodynamic Torque. T_H is the torque generated by the rudder when it is placed at some angle of attack other than zero, due to the fact that the center of pressure on a rudder does not coincide with the turning axis of the structure. The hydrodynamic torque is expressed as

$$T_H = \left(\frac{V}{V_0}\right)^2 (K_7\theta - K_8\theta|\theta|) \tag{11}$$

where V is the ship velocity, V_0 is the maximum ship velocity, and K_7 and K_8 are hydrodynamic torque load coefficients. By adjusting the values of K_7 and K_8, the hydrodynamic torque variation with rudder position can be adjusted to approximate almost any rudder design. If K_7 and K_8 are redefined, the above expression can be written in nondimensional form:

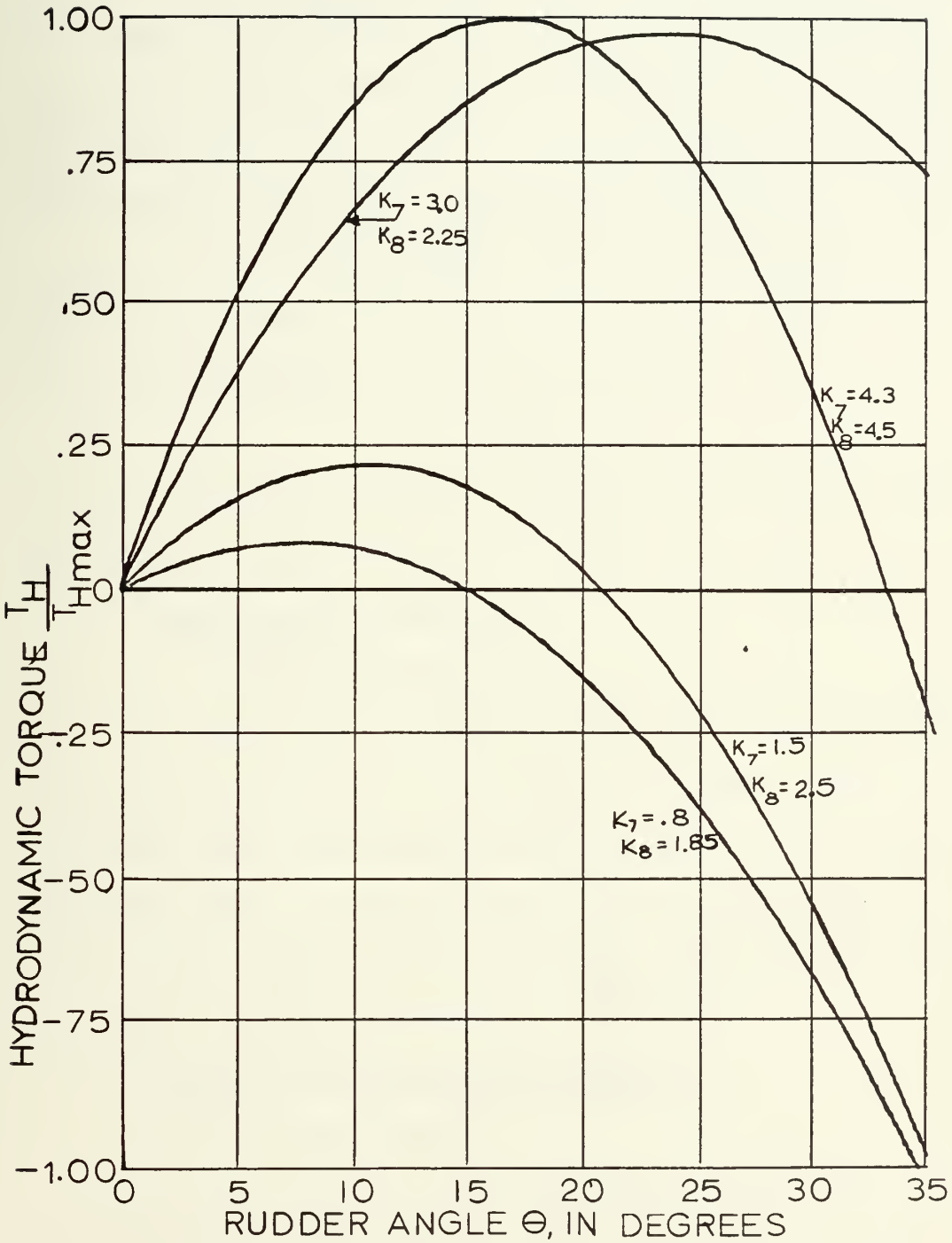

FIGURE 3
HYDRODYNAMIC TORQUE BEHAVIOR
FOR VARIOUS VALUES OF K_7 AND K_8

$$\frac{T_H}{T_{Hmax}} = K_7\left(\frac{\theta}{\theta_{max}}\right) - K_8\left(\frac{\theta}{\theta_{max}}\right)\left|\frac{\theta}{\theta}_{max}\right| \qquad (12)$$

where T_{Hmax} is the maximum hydrodynamic torque corresponding to V_0, and θ_{max} is the maximum rudder angle. See Figure 3 for curves of T_H/T_{Hmax} for varying values of K_7 and K_8. It can be seen that a variety of rudder torque characteristics can be simulated by adjustment of K_7 and K_8.

(3) Pressure Torque. The pressure torque T_p is the torque that is placed on the stock of the rudder by the hydraulic ram, through the connecting linkage. It can be expressed as

$$T_p = LAP_L \cos\theta \,, \qquad (13)$$

where L is the tiller length, A is the area of the actuator piston, and P_L is the load pressure drop.

2. Analog Computer Simulation

a. Hardware and Parameters

Figure 4 is a schematic diagram of the analog computer program which was designed to model the governing equations. Table I gives a list of typical system dimensions and other parameters which were used to set simulation values. Table II gives a list of the potentiometer settings for the values listed in Table I, and also lists the expressions which were used to develop the settings.

3. Discussion of the Baseline Simulation

a. Performance Curves

Examination of sample recordings obtained from the NSRDC showed that oscillations in velocity and pressure were present in the simulation outputs. The NSRDC indicated that the oscillation appeared to be a function of the inertia of the steering linkage, ram, and rudder, and of the system mechanical and hydraulic resiliences. Variation of

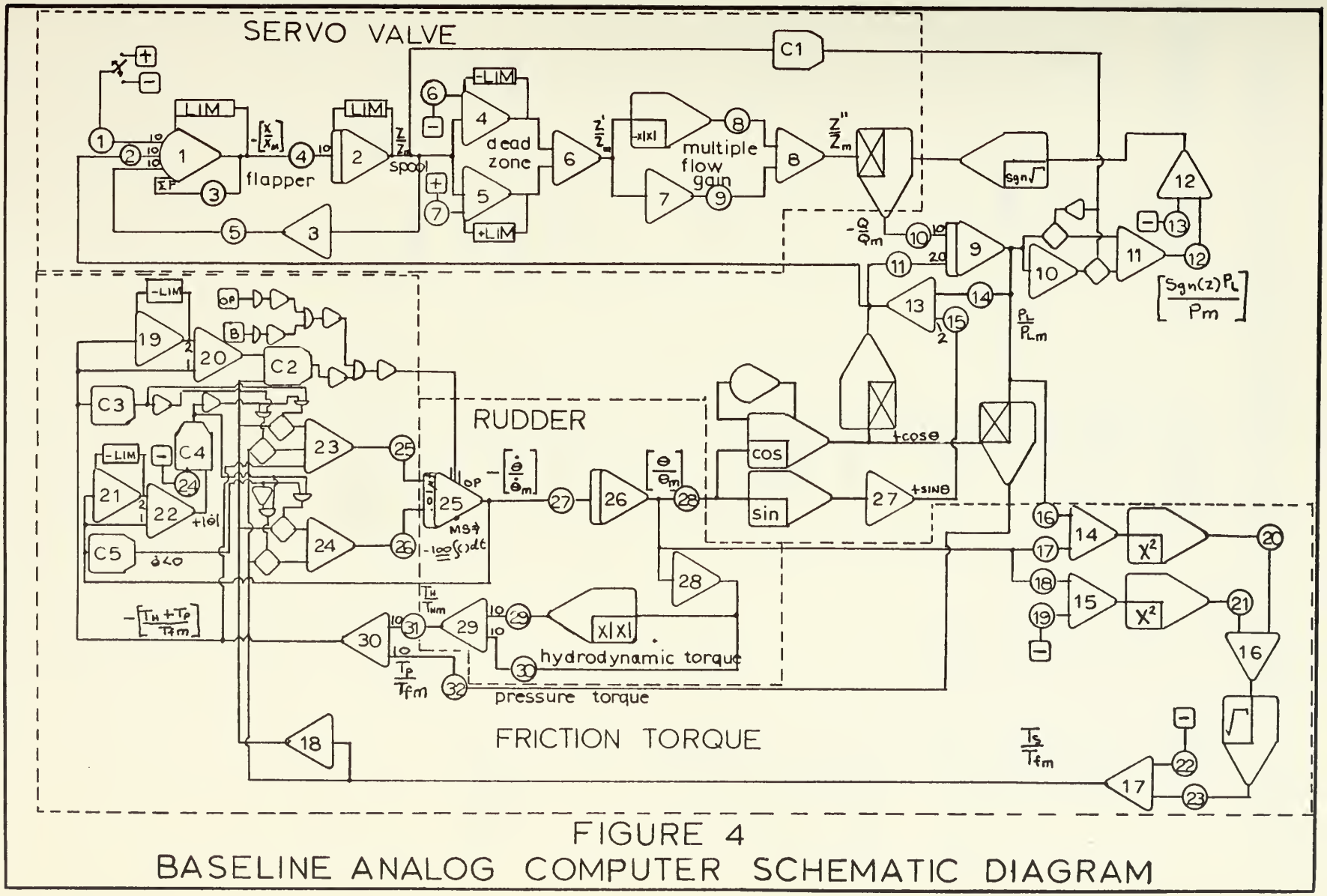

FIGURE 4
BASELINE ANALOG COMPUTER SCHEMATIC DIAGRAM

Table I

Submarine Steering System Parameters Used in the Baseline Simulation

Parameter	Value	Parameter	Value
A	80 in^2	L	30 in
C_d	.05	P_{max}	6,000 psi
db	.05	P_{Lmax}	3,000 psi
I	9100 in-lbf-sec^2	P_S	3,000 psi
K_1	.6	Q_{max}	278.86 in^3/sec
K_2	110	R	18 in
K_3	5.0	T_{Fmax}	$1.1661X10^6$in-lbf
K_4	375	T_{Hmax}	$3.93X10^6$in-lbf
K_5	7.20	T_{Pmax}	$7.2X10^6$in-lbf
K_6	0.015	W	25,000 lbm
K_7	1.5	X_{max}	.002 in.
K_8	2.5	y_{max}	17 in.
K_9	30,000	z_{max}	.5 in.
K_{10}	150,000	θ_{max}	35 degrees
K_{11}	3,000	$\dot{\theta}_{max}$	10 deg/sec.
K_{12}	800,000	β, time scaling factor	1

Table II

Potentiometer Expressions and Settings for Baseline Simulation
(See Fig. 4)

Potentiometer No.	Expression	Setting
1	$\frac{\theta_o K_1}{100 K_2 x_{max}}$	.9546
2	$\frac{\theta_m K_1}{100 K_2 x_{max}}$	.9546
3	Simulation Technique	.1
4	$\frac{K_4 x_{max}}{10 z_{max} \beta}$	.1500
5	$\frac{K_3 z_{max}}{100 K_2 x_{max}}$	.1136
6	db	.05
7	db	.05
8	multiple flow gain	.5
9	multiple flow gain	.5
10	$\frac{Q_{max}}{10\ K_6 P_L \beta}$ (1st footnote)	.406
11	$\frac{AL\dot{\theta}_{max}(\pi/180)}{20\ K_6\ P_{Lmax}\ \beta}$ (2nd footnote)	.4654
12	P_{Lmax}/P_{max}	.5000
13	P_S/P_{max}	.5
14	$\frac{AP_{Lmax}}{K_{12} y_{max}}$	.0177
15	$\frac{L}{2y_{max}}$	.8824

Potentiometer No.	Expression		Setting
16	$\frac{AP_{Lmax}}{3.45X10^5}$	(3rd footnote)	.6957
17	$\frac{K_{11}\theta_{max}}{3.45X10^5}$	(3rd footnote)	.3044
18	$\frac{K_9\theta_{max}}{1.075X10^6}$	(3rd footnote)	.9768
19	$\frac{W}{1.075X10^6}$	(3rd footnote)	.0233
20	$(3.45X10^5/1.129X10^6)^2$	(3rd footnote)	.6934
21	$(1.075X10^6/1.129X10^6)^2$	(3d footnote)	.9066
22	$\frac{K_{10}}{T_{Fmax}}$		.1286
23	$\frac{Cd\ R(1.129X10^6)}{T_{Fmax}}$	(3rd footnote)	.8714
24	ε		.0010
25	$\frac{T_{Fmax}}{100\dot{\theta}_{max}I}$		.1282
26	$\frac{T_{Fmax}(Tc/Ts)}{100\dot{\theta}_{max}I\beta}$		.1269
27	$\frac{\dot{\theta}_{max}}{\theta_{max}}$		.2857
28	$\frac{\dot{\theta}_{max}}{200}$	(4th footnote)	.1750
29	$\frac{K_8}{10}$		.25

Potentiometer No.	Expression	Setting
30	$\frac{K_7}{10}$	.15
31	$\frac{T_{Hmax}}{10\,T_{Fmax}}$	.3370
32	$\frac{T_{pmax}}{10\,T_{Fmax}}$	.6175

1. This expression was later found to be incorrect. See the text, Initial Investigation.

2. This expression was later found to be incorrect. See the text, Initial Investigation.

3. Numbers appearing in the numerators or denominators of these expressions represent scaling values calculated by the NSRDC.

4. Adjustment for SIN - COS generator design requirements.

these parameters modified the fundamental frequency of the oscillation, but did not eliminate it. It was found that the oscillation could be eliminated by the artificial introduction of viscous damping in the system, but only in much greater amounts than could be justified in view of apparent levels of viscous damping present in the actual system. No provision for viscous damping was included in the friction torque equation, since no source was immediately apparent in the structure.

b. Suspected Origins of the Oscillations

After some study of the baseline simulation, the NSRDC felt that the problem was located in either their recording equipment associated with their analog computer, in the mathematical models which had been developed, in settings of the simulator parameters, or in the basic assumptions used in the derivations of the governing equations, such as a lack of understanding of the available sources of damping in a submarine steering control system.

II. INITIAL INVESTIGATION

The initial investigation was conducted in order to gain a more complete understanding of the simulation, and to determine problem areas requiring extensive investigation. The baseline simulation was duplicated on a large analog computer, techniques and models currently used in simulating hydraulic control systems were studied, and information was gathered from personnel familiar with the baseline simulation development and submarine steering control systems. The baseline simulation was continually evaluated in terms of the information which had been gained, and several problem areas were found which required further analysis.

A. DUPLICATION OF THE BASELINE SIMULATION

The baseline simulation required duplication on local equipment in order to provide a check of the correctness of the programming completed at the NSRDC. The Naval Postgraduate School's COMCOR CI-5000 analog computer was used in this effort. The CI-5000 is a general purpose computing system, including analog, digital control, and patchable logic sections, and incorporates enough components of various types to accommodate the baseline simulation.

The writer first attempted to directly adapt the baseline simulation analog schematic directly to the CI-5000, adjusting the simulation only to compensate for CI-5000 peculiarities, thereby assuming that the equations and potentiometer expressions of the baseline simulation were correct, and that the analog schematic diagram accurately modeled the governing equations. This first attempt was unsuccessful; analog components rapidly overloaded, and the system failed to reproduce the sample curves that the baseline

simulation at the NSRDC had produced when operated under identical conditions. It appeared that the baseline simulation's governing equations, potentiometer expressions, and analog programming required detailed checking for mathematical and functional correctness.

The governing equations were found to be consistent with the sign conventions evidently adopted by the developer (See Figure 1), with the exception of equation (7),

$$Q = -A\dot{y} + K_6\dot{P}_L \ .$$

Examination of the geometry of the system (Figure 1) revealed that the sign of the $\dot{y}$ - term should have been positive, since a positive flow rate would cause a positive change in y, if the pressure drop P_L were held constant. Also, for a zero flow condition (Q = 0) a positive change in y would result in a negative change in the pressure drop. Thus, equation (7) should have read

$$Q = A\dot{y} + K_6\dot{P}_L \ . \qquad (7a)$$

The NSRDC later confirmed that this was the case.

Potentiometer expressions were found to be consistent with the baseline simulation schematic diagram and the governing equations, with the exception of potentiometers 10 and 11, which were associated with integrator 9 of the baseline simulation (Figure 4). A term in the denominator of each potentiometer expression apparently had been dropped; the denominators should have read $10(P_{Lmax})[K_6+(A^2/K_{12})]$ instead of $10(K_6P_{Lmax})$ and $20(K_6P_{Lmax})$ for pots 10 and 11, respectively. The need for the additional term in each expression's denominator was later confirmed by the NSRDC. The additional terms modified the values of the two potentiometers significantly;

the value of pot 10 changed from 0.6197 to 0.4060; the value of pot 11 changed from 0.4654 with a gain of 20 on integrator 9 to 0.6060 with a gain of 10. This resulted in an effective reduction of the system hydraulic compliance and in a change of the overall characteristics of the pressure torque. Tests later showed that the omission of these coefficient terms was the primary reason for the initial failure to duplicate the baseline simulation.

Except for the two potentiometer settings, the analog program (Fig. 4) appeared to accurately represent the verified governing equations. Accordingly, another attempt was made to adapt the program to the CI-5000. Only slight deviations from the baseline schematic diagram were necessary in order to accommodate the CI-5000 component peculiarities.

When the adapted baseline simulation was operated under the potentiometer conditions listed in Table II, with the exception of pots 9 and 10 which were set as previously modified, the system behaved in the same manner as it had during operation at the NSRDC. Oscillations identical to baseline forms were observed in $\dot{\theta}$ and P_L (Figure 5). As a result of this duplication of performance, using several different types of recording equipment that exhibited varying response characteristics, it appeared that the recording equipment at the NSRDC was not the source of the oscillations. Further, since all errors in mathematics and in the settings of the simulator parameters required correction before the baseline performance could be successfully duplicated, it appeared that the errors which were found were the result of faulty communication of the baseline simulation to the writer, and were not present in the program used to generate the sample curves. Apparently, then, the mathematical models were consistent in sign conventions and had been manipulated correctly in the development

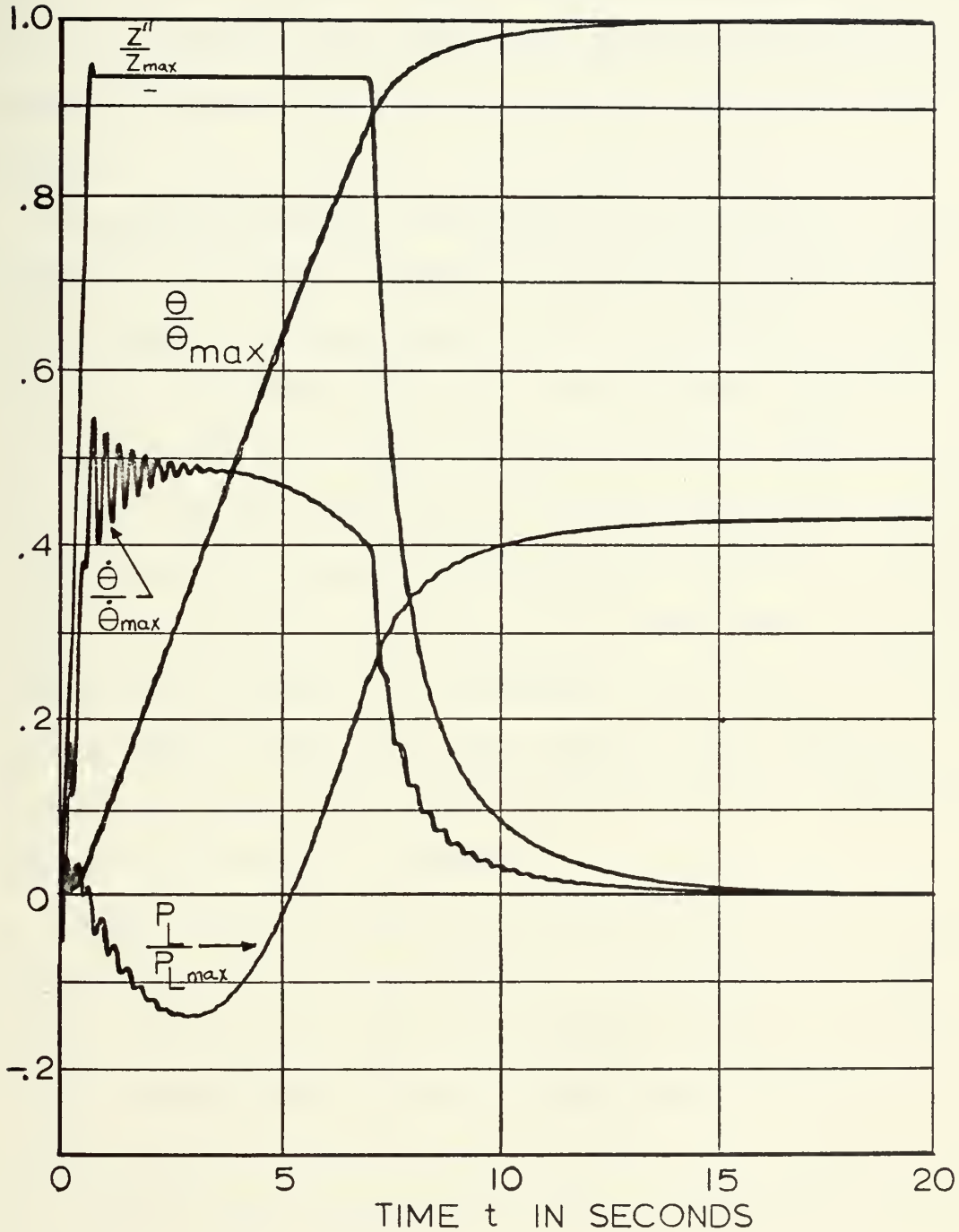

FIGURE 5

BASELINE SIMULATION RESPONSE
θ_o = 35 DEGREES

of the analog board, the potentiometers were correctly scaled, and the analog wiring was correct. Thus, the simulation appeared to be correct within the framework of the fundamental assumptions involved in the mathematical formulations; however, the oscillations were still present in the output.

Two situations seemed to be possible. First, perhaps the oscillations evidenced in the NSRDC data were not representative of the behavior present in real submarine steering systems, and the simulation was therefore inadequate. This situation could have occurred because fundamental errors or omissions were made during the formulation of the baseline simulation governing equations, say by the use of faulty assumptions regarding the significance of one or more physical processes present in a steering system. The situation could also have occurred because system materials, dimensions, and properties were improperly represented in the development of the numerical values used in the "typical" system simulation, by the inclusion of inconsistent units conversions, unrealistic dimensions, or faulty physical materials constants.

Second, perhaps the oscillations appearing in the NSRDC data were representative of real system behavior, and the difficulty had its origins in the harboring of an incorrect knowledge of the actual performance of a ship's steering control system. No actual system recordings were submitted with the baseline simulation, and therefore no immediate comparison was possible between the simulation performance and real conditions in the system.

B. BACKGROUND INVESTIGATION

1. Study of Currently Used Models

Assuming that the oscillations observed in the baseline simulation were not representative of real steering system behavior led to a background investigation of techniques and models currently used in simulating hydraulic systems in order to develop a clear knowledge of the fundamental assumptions made during the development of the baseline simulation. This background examination consisted of studies in the hydraulic controls field, and communication with personnel familiar with the simulation and ship steering control systems.

The search for currently used models and techniques produced several results. It was found that servovalves were usually designed so that they were the controlling element in hydraulic systems. However, in the baseline simulation, any error signal representing more than four degrees resulted in saturation of the control valve, resulting in the servovalve having no variable control over the velocity of the load, until the error signal again fell below a value representing four degrees. Thus, the servovalve was virtually being used as an open-shut valve much of the time. The presence of deadband and multiple flow gain in the valve tended to reduce the sensitivity of the valve to small errors, and to increase it for errors in excess of four degrees, thus heightening the effect.

It was also noted that if the expressions for the baseline simulation were transformed into Laplace notation, and deadband and multiple flow gain effects were temporarily neglected, the resultant expression would be

$$Z(s) = \left(\frac{K_1/K_2}{s+K_3/K_2} \right) E(s) \qquad (14)$$

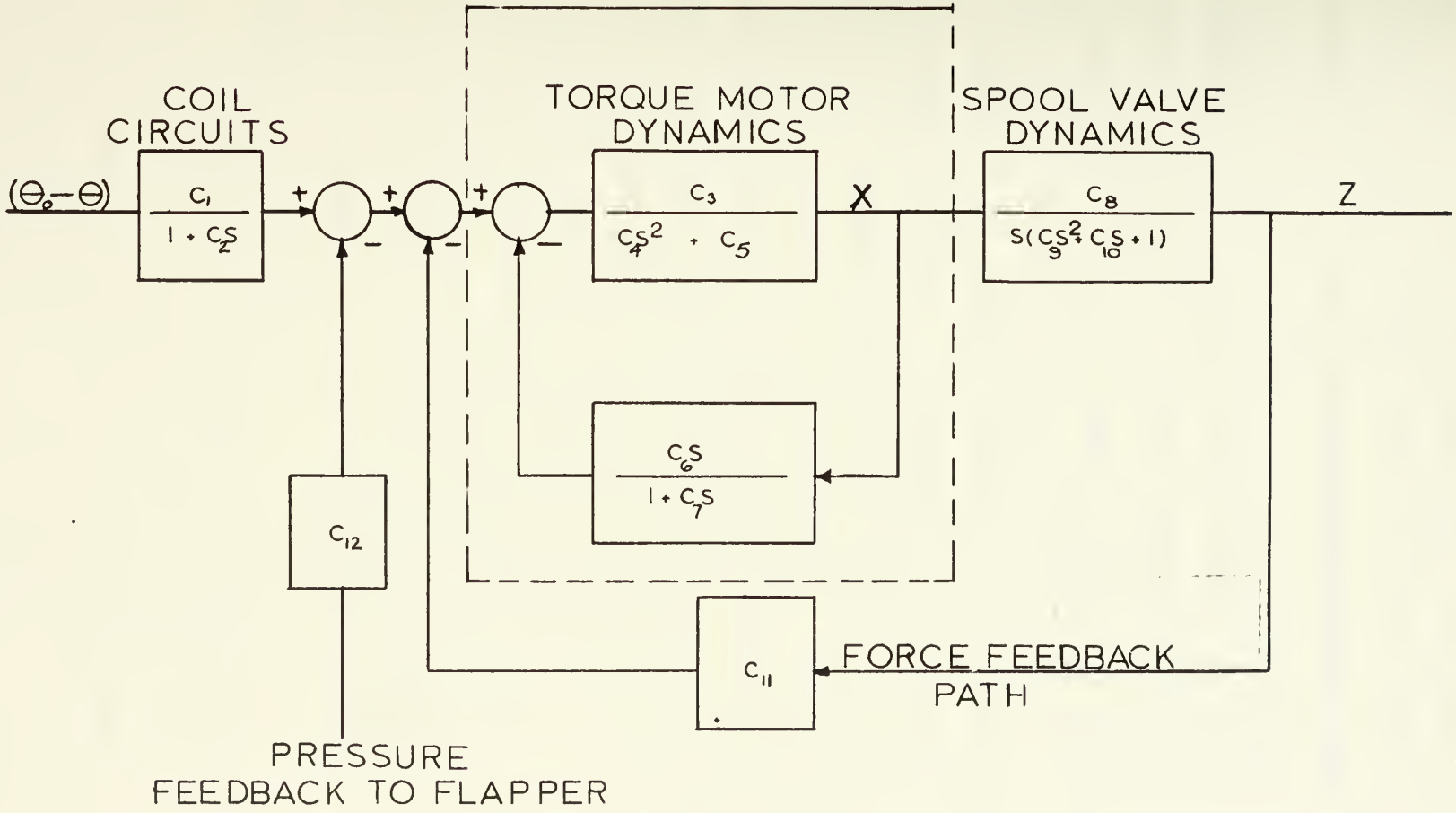

FIGURE 6
BLOCK DIAGRAM OF A TWO-STAGE SERVOVALVE
WITH FORCE FEEDBACK

where Z and E represent the Laplace-domain variables for z, the valve spool position, and e, the error signal, respectively, and s is the Laplace transform variable. This function was identical to one developed by Morse [1] for a valve incorporating centering springs instead of force feedback, for use in systems where the load was assumed to be very small compared with the available hydraulic power. The actual valve being used, however, consisted of a two-stage, force-feedback design being used to control a load of the same order of magnitude as the available hydraulic power [2]. Merritt [3] developed a transfer function block diagram for a two-stage, force-feedback servovalve, which incorporated the general form shown in figure 6. A vast degree of simplification of Merritt's expression obviously would have been necessary in order to arrive at the expression used in the baseline simulation. Quite possibly, the coefficients indicated by Merritt in many instances were of such magnitudes that their effects were not important in the actual performance of submarine steering system servovalves, since high frequency effects would become unimportant when other system frequencies were quite low. Furthermore, the pressure feedback to the flapper valve that Merritt included in his expression was possibly unimportant in this particular case. However, it seemed advisable to check the numerical value of each term in the detailed expression, in order to evaluate the validity of the baseline simulation's expression.

Through communication with Mr. Guy Johnson [4], the developer of the baseline simulation, it was learned that many of the servovalve design values, needed to calculate the coefficients in the Merritt block diagram, were difficult to obtain. It was also found that the expression used in the baseline simulation had been developed by a combination of experimental

and intuitive means, and that the servovalve simulation was considered to be sufficiently accurate for the particular design studies in which it would be used. Finally, it was determined through observations of the performance of the adapted simulation program that the oscillations did not appear to be affected by the servovalve action. Thus, further investigation of the validity of the servovalve simulation did not appear to be justified until the origin of the oscillations had been fully investigated.

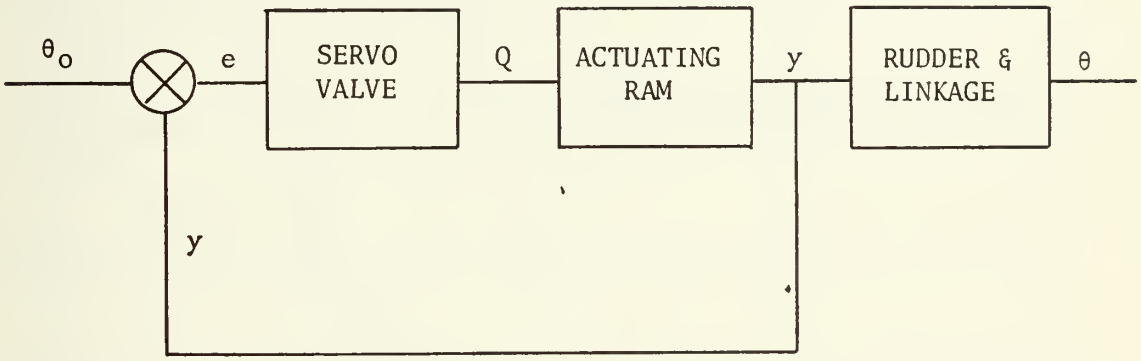

Figure 7. Functional Block Diagram of a Submarine Steering System

Figure 7 is a functional block diagram of a submarine steering control system. The control system was not entirely closed loop in construction, since the error signal controlling the function of the servovalve was generated by the ram position rather than by the actual rudder position. This placement of the feedback element was consistent with established design practice [5], since the inclusion of the compliant structure of the rudder and linkage within the servo loop could result in significant instability problems. Additionally, an electrical feedback element located outside the pressure hull of a submarine, in a location

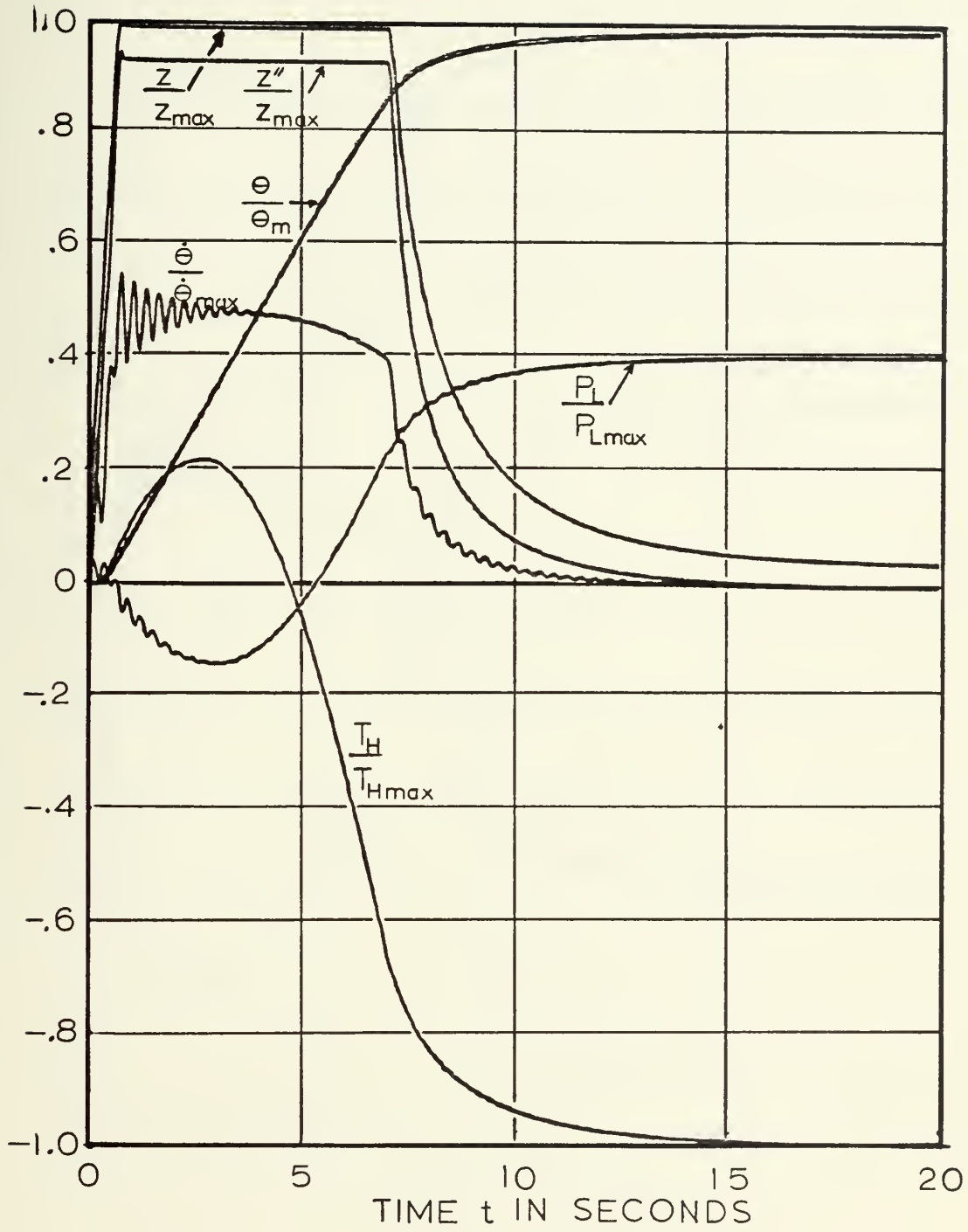

FIGURE 8
CURVES OF SEVERAL PARAMETERS
OF C1-5000 SIMULATION

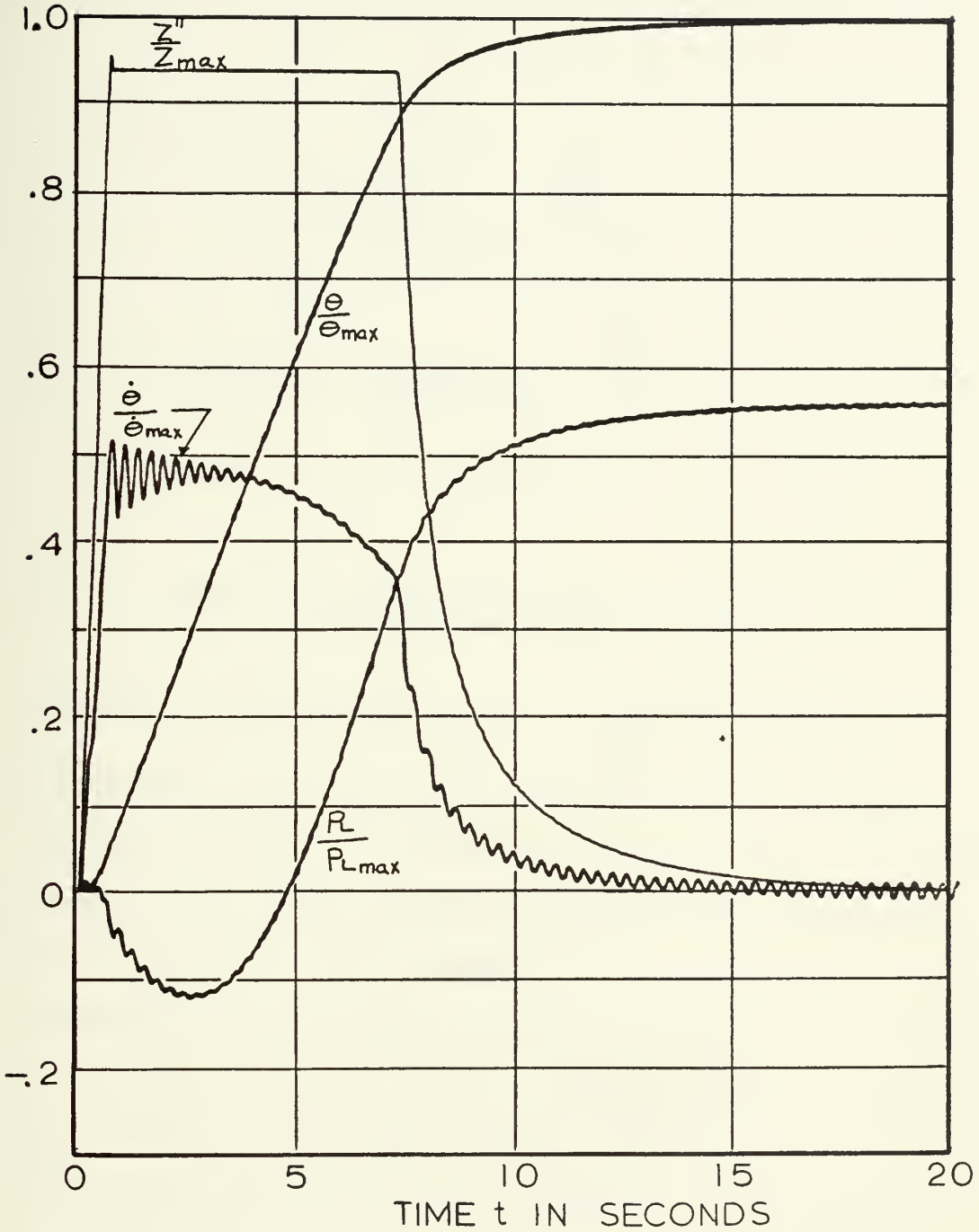

FIGURE 9
"FRICTIONLESS" LOAD CONDITION, $T_F = 0$.

flooded with sea water, would pose several design problems, including the need for increased reliability due to its inaccessability when at sea.

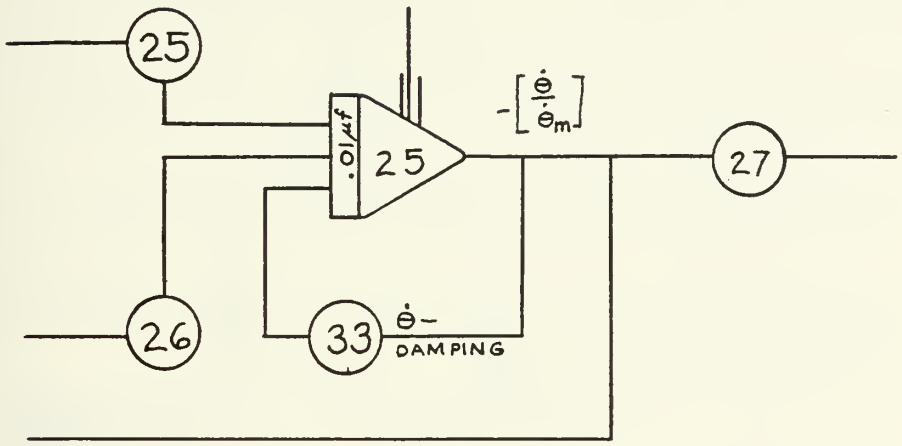

Figure 10. Circuit Modification of Fig. 4, Introduction of Viscous Damping

Examination of the curves for $\frac{\theta}{\theta_m}$, $\frac{\dot{\theta}}{\theta_m}$, $\frac{P_L}{P_{Lm}}$, $\frac{T_H}{T_{Hm}}$, $\frac{z''}{z_m}$, $\frac{y}{y_m}$, and $\frac{z}{z_m}$ (Figure 8) generated by the CI-5000 simulation revealed that the oscillations were present only in the linkage and the load portions of the simulator. Manipulations of the baseline simulation friction coefficients failed to eliminate or modify the effect, although total exclusion of any friction in the system resulted in very small undamped oscillations in θ, and appreciable oscillations in $\dot{\theta}$ and P_L after the control surface had essentially reached the desired position (see Figure 9). Further tests showed that small values of negative feedback across integrator 25, which were introduced through the use of the circuit modification indicated in Figure 10, resulted in elimination of the oscillations. This feedback across the integrator would be representative of damping in an actual system containing such elements as dashpots. With no other friction in the system, a feedback level of 0.005 $\frac{\dot{\theta}}{\theta_m}$ was sufficient to eliminate the limit cycle.

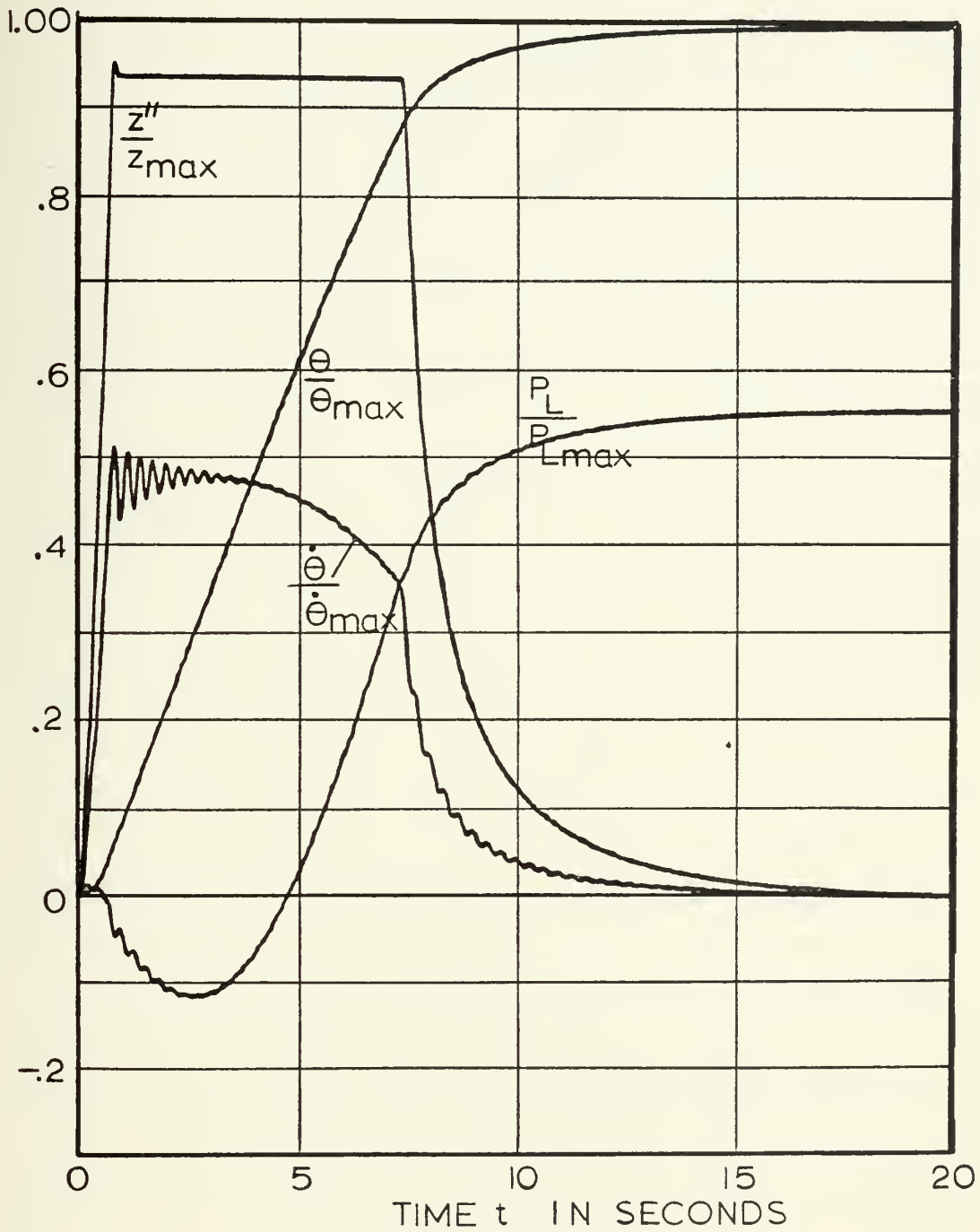

FIGURE 11
VISCOUS DAMPING LEVEL .005$\frac{\dot{\theta}}{\dot{\theta}_{max}}$,
$T_F \equiv 0.$

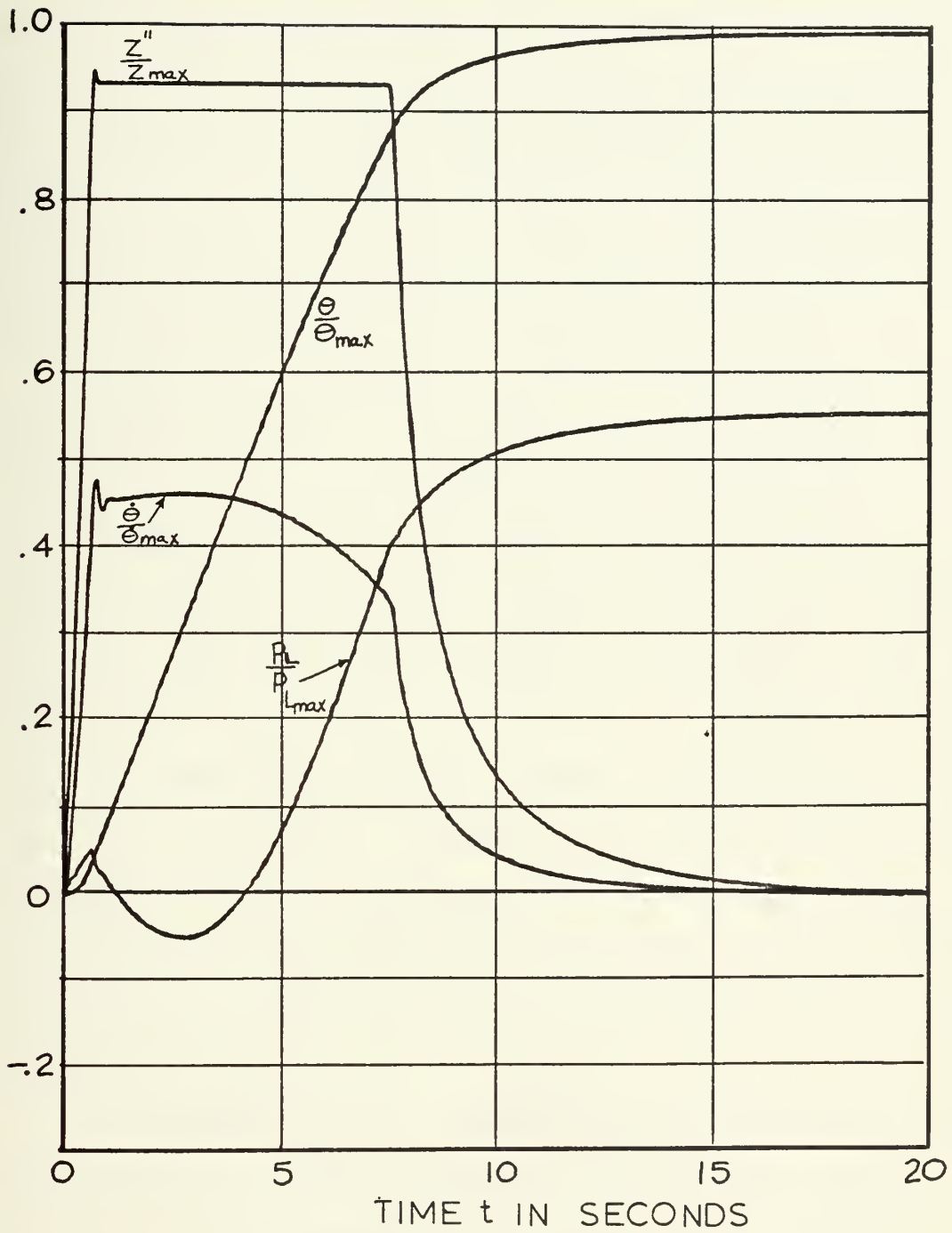

FIGURE 12

VISCOUS DAMPING LEVEL .12 $\frac{\dot{\theta}}{\dot{\theta}_{max}}$, $T_F = 0.$

Furthermore, feedback levels of 0.12 $\frac{\dot{\theta}}{\dot{\theta}_m}$ were sufficient to approach a critically damped condition in the load and linkage simulator. (See Figures 11 and 12.) If friction levels present in the baseline simulation were programmed into the CI-5000, approximately the same value of $\dot{\theta}$ -damping as in the frictionless configuration was required to produce critically damped behavior, while the sustained limit cycle was eventually eliminated by the presence of the baseline friction itself.

Damping terms proportional to $\dot{\theta}$ were totally absent from the baseline simulation equations. Intuitively, however, some damping would be present in any system in which viscous fluids such as sea water are displaced by moving objects, since work must be expended to keep objects moving at a constant rate, whether linearly or rotationally, through a real fluid. Thus, the neglect of damping in the linkage and rudder portion of the simulation did not appear to be realistic. A superficial examination of the system did not reveal any large sources of damping, or even sources which would provide a fraction of that needed to approach a critically damped condition in the linkage. Anticipating that a lengthy investigation of system damping would be necessary, the writer identified this area as requiring first priority for further investigation, and postponed further analysis of it.

Correspondence with Mr. Johnson resulted in the writer receiving some drawings of a 671-class submarine's steering control system [7]. Examination of these drawings revealed that functional concepts of several features of the design had undergone considerable alterations in the process of the development of the idealized model. A compensated actuator had been assumed in the simulation development; i.e., equal areas had been assumed on both sides of the actuator ram (Figure 1). Examination

of the drawings, however, and discussion with Mr. Johnson revealed that the actuator on a typical submarine was in reality uncompensated; i.e., unequal areas were available on opposite sides of the actuating ram piston. The writer was informed, however, that the difference in performance parameters due to the neglect of the unequal areas was not of major concern in the overall reasons for simulating the steering system.

Further study of the drawings revealed that the crosshead configuration had been simplified in such a manner that it was no longer representative of the actual design. The crosshead, originally assumed to operate in a sleeve open at both ends, Figure 1, was in reality supported by a sleeve open at only one end in most submarine designs, Figure 13. The effect of this variation in the crosshead configuration could only be determined through a detailed knowledge of the dimensions, design, and clearances involved in an actual crosshead, and these parameters could not be gleaned from the drawings that the writer had available. Further investigation of the crosshead influence on the system seemed to be justified, since the assembly resembled a dashpot in appearance, and possibly was capable of providing the source of damping which seemed to be needed in the system. Consequently, a detailed analysis of the effect of a typical crosshead structure on steering system performance seemed to be in order, and was identified as an area for further work.

2. Verification of Typical System Values

Several nondimensional coefficients, load parameters, and properties had been used to develop the simulation, such as the hydraulic resilience coefficient, the rudder mass, and inherent materials properties. Inaccurate development of system numerical values could have contributed the system oscillations. Attempts were made to determine the values of many of these

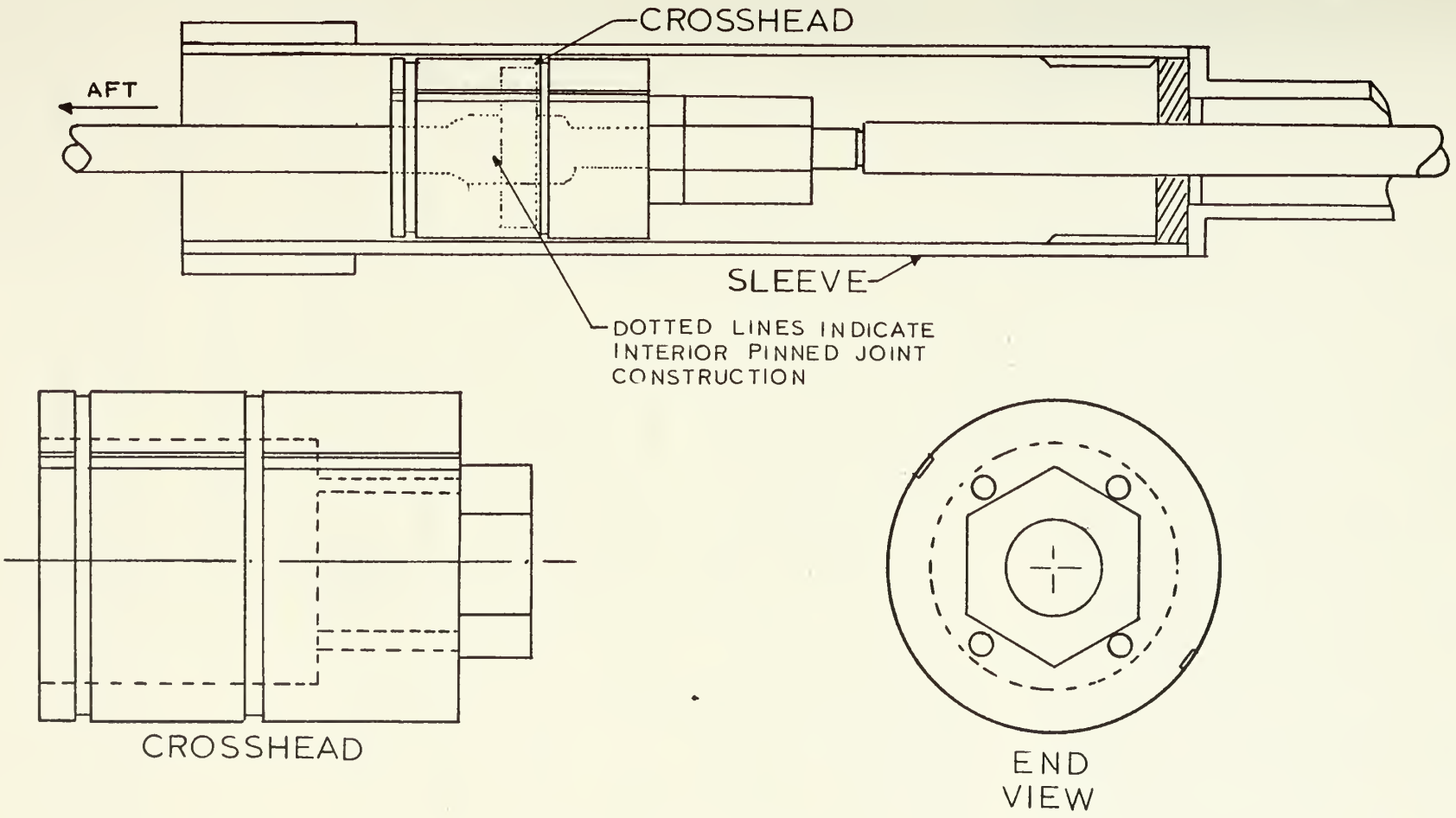

FIGURE 13
TYPICAL CROSSHEAD DESIGN

constants from basic principles, but the effort was thwarted due to a lack of information regarding dimensions, physical constants, system construction details, and algebraic expressions for any of the nondimensional constants K_1 through K_{12}. It became apparent that much time could be spent trying to determine the validity of each derived constant without having the appropriate algebraic expression available for examination. Therefore, this possible source of inaccurate system simulation was identified for further investigation, and was set aside.

3. Actual System Performance

Actual system recordings of θ, $\dot{\theta}$, and P_L were mentioned by Mr. Johnson as not demonstrating the oscillations found in the simulation. The writer requested that such recordings be forwarded to him in order to gain a first-hand knowledge of the actual system performance, but was unsuccessful in obtaining any such recordings. Without any more information about the actual system performance than the available qualitative description of the behavior, no reasonable conclusions could be reached about the actual system performance. Because an accurate representation of a system could not be claimed until a favorable comparison with accurate actual system performance could be accomplished, it was felt that such a determination of steering system performance would be beneficial, and the subject was identified as requiring further investigation.

C. SUMMARY OF THE INITIAL INVESTIGATION

1. Conclusions

As a result of the duplication of the baseline simulation, and subsequent experiments performed with the program, the following conclusions were reached:

(1) The recording equipment at the NSRDC had accurately recorded the performance of the simulation, and was not the source of the oscillations.

(2) The equations and potentiometer settings were consistent within the framework of the fundamental assumptions involved in the simulation's mathematical development.

(3) The oscillations were confined to the load portion of the simulator, and did not appear to be sustained by overall system instability.

(4) A negative feedback level of 0.005 $\frac{\dot{\theta}}{\dot{\theta}_m}$ was sufficient to eliminate the limit cycle oscillation, and 0.12 $\frac{\dot{\theta}}{\dot{\theta}_m}$ achieved a critically damped condition, in the load simulation under otherwise frictionless conditions. A negative feedback level of 0.12 $\frac{\dot{\theta}}{\dot{\theta}_m}$ was also sufficient to create a critically damped condition in the load simulator under baseline friction conditions.

Studies, and communications with personnel familiar with the simulation and with actual submarine steering control systems, led to the following conclusions:

(1) The servovalve equation used in the baseline simulation was not developed to completely model either the type of servovalve used in the real system under study, or the type of load which was present in the actual system. The net effect of the substitution of a simple expression for a complicated one was not immediately determined, except that it did not appear to affect the system load oscillations.

(2) The actuator had been modeled in the system simulation as a compensated ram, rather than being modeled as the uncompensated actuator used in real systems. Although the effect of this simplification

on the system was unknown, communication with experienced personnel seemed to indicate that the effect was unimportant.

(3) The actual crosshead design had been modeled in such a way that damping effects possibly present in the component were not taken into account. Further study seemed warranted.

(4) Viscous damping effects in the load had been totally ignored in the development of the simulation, although such effects controlled the unwanted system oscillations, and normally would be present to some degree in any system incorporating the movement of structures through real fluids. A search for viscous damping sources in the load was assigned first priority for extensive investigation.

(5) The origins of many of the nondimensional constants used in the simulation were obscure, and efforts to verify their correctness were unsuccessful, due to the lack of appropriate algebraic expressions, dimensions, and materials constants.

(6) Actual documentation of real system performance in the situations being modeled appeared to be vague and incomplete. Little information was available concerning the actual response characteristics of submarine steering control systems to step inputs. An extensive investigation of real system performance appeared to be necessary.

III. LOAD AND LINKAGE DAMPING

Of the areas identified in the initial investigation as requiring further research, only the search for sources of linkage and load damping was pursued in the present investigation. Analysis of the submarine system identified three locations where damping might possibly be present: the system's dynamic seals and bearings, the crosshead structure, or the rudder itself. No other components appeared to be designed in such a manner that they could possibly produce an appreciable quantity of damping.

In order to determine levels of damping in the various components, detailed information was needed concerning dimensions, clearances, materials, constructions, and lubrication for the linkage parts and rudder. The writer was referred [8] to Mr. Leeland Smith [9] of the Mare Island Naval Shipyard, who provided detailed drawings of the steering control system for the SSN 671 class submarine.

A. BEARINGS AND DYNAMIC SEALS

The possibility was considered that the expressions employed for the friction present in the bearings and dynamic seals (equations 9 and 10) were not representative of the actual processes present in the submarine system, and that the inherent friction of the bearings and seals was better described as displaying viscous behavior.

Keller [10] indicated that compression packings, such as those used at the pressure hull penetration and the actuator-piston rod interface, are normally lubricated by allowing very slight amounts of leakage past the seal. Examination of the SSN-671 drawings revealed that the pressure hull packing was additionally lubricated with grease. Despite these indications

that viscous effects could be present in these seals, discussions with Mr. Smith, William Kendall [12], and Leonard Chase [12] of the Mare Island Naval Shipyard resulted in the writer's learning that friction in such seals was best approximated as sliding friction, since friction loads were normally observed to be fairly independent of actuator rod velocity, due to the velocities and allowable leakage rates present in the system. Thus, the baseline model of seal friction appeared to be justified.

Study of the rudder bearings seemed to support the use of the baseline simulation's bearing friction expressions. The large rudder weight, combined with hydrodynamic loads, small rates of rotation present in the rudder stock, and the ill-defined lubricating qualities of sea water, resulted in enough analytical uncertainties being present to discourage any attempt to model such bearings as either slipper-type or journal-type surfaces. Again, the baseline simulation expression seemed to provide a bearing surface description that probably was as accurate in magnitude and parameter dependence as any other expression that could be analytically developed using known conditions and existing lubrication theory. Experimental and analytical work of a scale beyond the scope of this project could prove useful in future design work involving bearings and seals of the types present in the submarine system.

B. CROSSHEAD

1. General Description

Examination of the SSN-671 drawings, and discussions with Mssrs. Smith, Kendall, and Chase concerning general construction details of crossheads, revealed that, as a rule, crossheads somewhat resembled dashpots in construction, due to their piston-in sleeve arrangements, and their free-flooded nature. Provisions were normally made in the construction of

crossheads to eliminate any possible damping effect by the drilling of large holes through the piston portion of the structure. Because damping sources were being sought, the writer decided to analyze the crosshead in order to determine what damping effects, if any, were present.

Figure 13 shows a crosshead design based on information taken from the SSN-671 drawings. The crosshead consists of a partially bored out cylinder 19 inches in length, with a diameter of 11.986 inches, and four one-inch I.D., eight-inch in length holes axially bored through the solid head of the piston. This piston rides in a twelve-inch I.D. tube, typically sealed along its length except at the rear end, which is open to allow the passage and free rotation of the link connecting the actuator shaft extension and the rudder tiller. The piston incorporates several lock-preventing 0.75 in. X 0.125 in. circumferential grooves, and two 0.125 in. X 0.5 in. axial slots along the outside radius. As a result of the radial clearance between the piston and the sleeve, the slots, and the holes in the crosshead, the entire sleeve is free flooded, and flow of sea water past the crosshead must take place as it is moved in and out of the sleeve.

2. Assumptions

In approximating the behavior of the flow past the crosshead and the viscous drag associated with that flow, it was assumed that the fluid velocities through the holes, slots, and radial clearance of the crosshead were considerably greater than the motion of the piston relative to the sleeve, thereby implying the existence of fixed orifices of irregular shape. Laminar flow was also assumed.

3. Equations

a. Eccentric Piston in a Sleeve

For an annulus formed by a solid eccentric cylinder in a sleeve with no relative movement involved, the flow rate Q_c can be expressed as [13]

$$Q_c = \frac{\pi r c^3}{6\mu l}\left[1 + \frac{3}{2}\left(\frac{\varepsilon}{c}\right)^2\right]\left(P_1 - P_2\right) \tag{15}$$

where r is the radius of the sleeve, μ is the absolute viscosity of the fluid, l is the length of the tube, ε is the eccentricity of the piston with respect to the center of the sleeve, and (P_1-P_2) is the pressure drop across the length of the tube.

b. Laminar Flow Through Rectangular Passages

For the slots [13],

$$Q_s = \frac{wh^3}{12\mu l}\left[1 - \frac{192h}{\pi^5 w}\tanh\frac{\pi w}{2h}\right] \tag{16}$$

where w is the width of the slot, h is the depth, and all other symbols retain their previous meanings.

c. Flow Through Short-Tube Orifices

Merritt [14], combining the work of Langhaar [15], Kreith [16], and Shapiro [17], developed an expression for the flow rate Q_0 through short tube orifices:

$$Q_0 = C\,A'\left[\left(\frac{2}{\rho}\right)\left(P_1 - P_2\right)\right]^{1/2} \tag{17}$$

$$C = \begin{cases} \left[1.5 + 13.74\left(\frac{1}{DRe}\right)^{1/2}\right]^{-1/2} & \frac{DRe}{l} > 50 \\ \left[2.28 + 64\left(\frac{1}{DRe}\right)\right]^{-1/2} & \frac{DRe}{l} < 50 \end{cases} \tag{18}$$

where C is the loss coefficient, ρ is the fluid density, D is the hole diameter, Re is the Reynolds Number based on the mean velocity of the flow in the tube and the hole diameter, and all other variables retain their previous meanings. If equations 15, 16, and 17 are manipulated

briefly, the pressure drop P_1-P_2 can be expressed as a function of the flow rate Q_0, the kinematic viscosity ν, D, and ρ:

$$P_1-P_2 = \left[\frac{8\rho}{\pi^2 D^4}\right] Q_0^2 \begin{cases} 1.5+6.87\sqrt{\frac{\pi\nu l}{Q_0}} & Q_0 > 12.5\pi\nu l \\ 2.28+\frac{16\pi\nu l}{Q_0} & Q_0 < 12.5\pi\nu l \end{cases} \quad (19)$$

If a total mass balance is made across the crosshead, it is found that

$$A_{CH}\,\dot{y} = MQ_0 + NQ_S + Q_C \quad (20)$$

where A_{CH} is the cross-sectional area of the crosshead, M is the number of holes in the crosshead, and N is the number of slots.

The force caused by the pressure difference across the crosshead can be expressed as an equivalent torque T_{CH} at the rudder pivot, by multiplying the crosshead force $F_{CH} = A_{CH}(P_1-P_2)$ by the length L of the tiller arm:

$$T_{CH} = A_{CH}\, L\, (P_1-P_2) \quad (21)$$

Figure 14 shows curves of T_{CH} versus $\dot{y}$ generated through the solution of equations (18) -(20) using the previously listed crosshead dimensions, ρ equal to 64 lbm/ft^3, and ν equal to 1.41 X 10^{-5} ft^2/sec (water at 50 degrees F), for various sizes of piston holes, assuming four holes and two slots, and an eccentric piston in the sleeve. To generate the curves, equations (18) and (19) were solved for P_1-P_2 as a function of Q_0. Then Q_S and Q_C were calculated, and appropriate multiples of Q_0, Q_S, and Q_C were used in accordance with equation (20) to produce $\dot{y}$. Equation (21) was then used to determine T_{CH}.

For any crosshead incorporating four holes any larger than 0.1 inches in diameter, it was found that zero pressure differential existed. As the diameter of the holes was decreased, with the dimensions and number

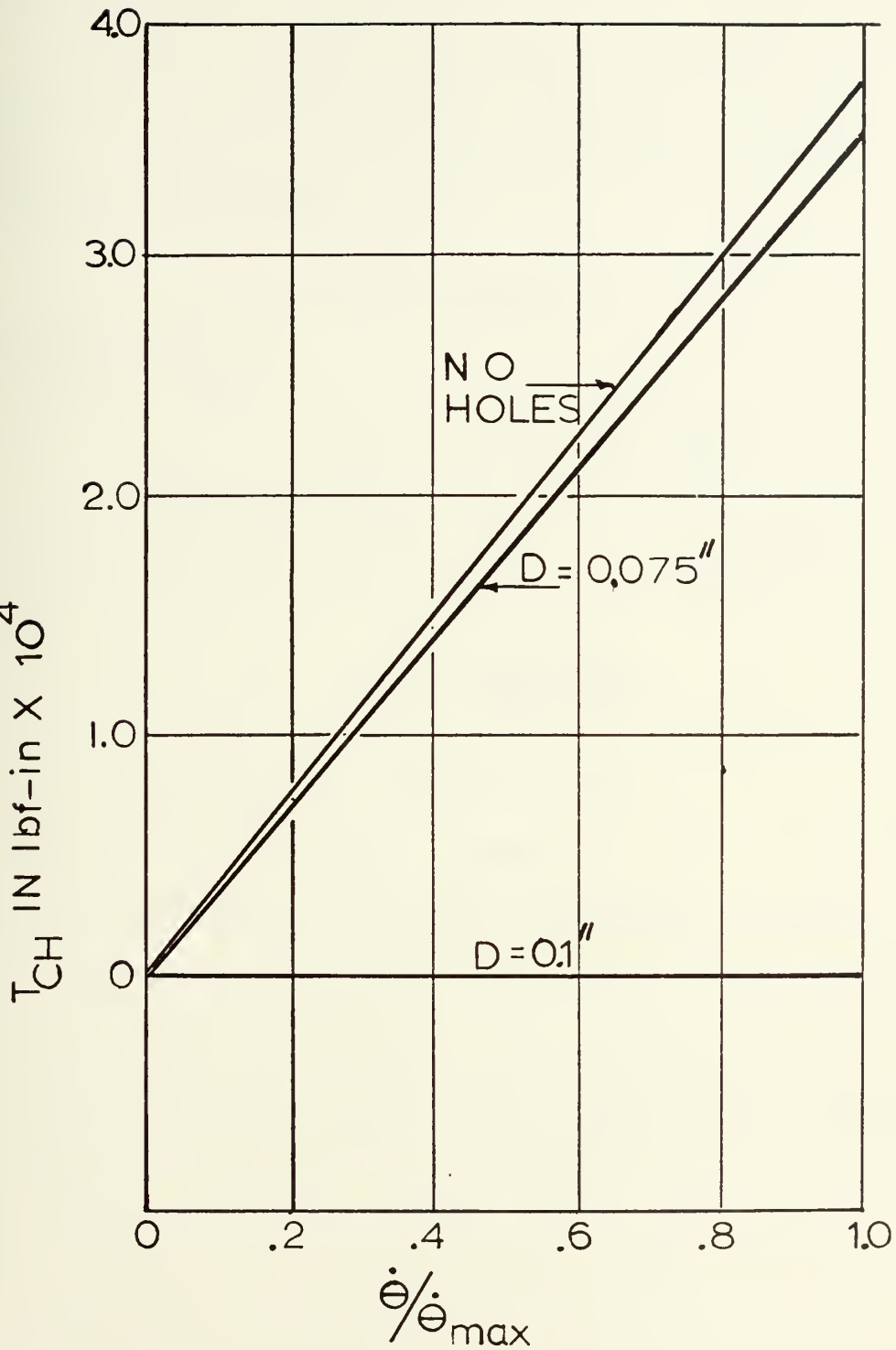

FIGURE 14
CROSSHEAD TORQUE
FOR VARIOUS HOLE SIZES

of slots and the parameters for the annulus remaining constant, a pressure differential began to exist across the structure. Finally, as the holes were eliminated, (P_1-P_2) approached levels sufficient to create significant values of T_{CH}. For the values of the zero-holes curve used in Figure 14, T_{CH} could be expressed as

$$T_{CH} = 7.48X10^3\dot{y} \tag{22}$$

or, since $\frac{\dot{y}}{\dot{y}_m} \sim \frac{\dot{\theta}}{\dot{\theta}_{max}}$,

$$T_{CH} = (7.48X10^3\dot{y}_{max})\left(\frac{\dot{\theta}}{\dot{\theta}_{max}}\right) \tag{23}$$

If the above equations were scaled for introduction into the simulation, potentiometer 33 would be set according to the expression

$$a_{33} = \frac{7.48X10^3\dot{y}_{max}}{100\ I\dot{\theta}_{max}} \tag{24}$$

For I = 9100, and $\dot{y}_{max}$ = 5 inches per second,

$$a_{33} = .00412.$$

Since this value of the potentiometer represented the maximum available T_{CH}, it was seen that the actual effect of the crosshead on the system damping was very small. In fact, using one-inch diameter holes would make the crosshead damping essentially zero. However, since a feedback level of $.005\ \frac{\dot{\theta}}{\dot{\theta}_m}$ was previously found to be sufficient to eliminate limit cycles in the "frictionless" system simulation, $.00412\ \frac{\dot{\theta}}{\dot{\theta}_m}$ could assist other small sources in the damping of the oscillations in the baseline simulation. Although the results of the investigation of the crosshead damping were less spectacular than had been desired originally, since the $\dot{\theta}$- feedback sufficient to create a critically damped condition in the load had not been justified, the author felt that the identification of a small source of damping had

been achieved, that identification possibly proving to be of some worth in future design work if a small amount of damping somehow proved necessary.

Some argument could have been made that further modification could create more damping. However, for this to be done, the system would need to be sealed at both ends, due to the approach of P_2 to the vapor pressure of water in the contained volume when the crosshead was moving out of the tube. Of course, the open end of the crosshead sleeve was not capable of being closed, due to the primary function of the crosshead, which was to provide a portion of a slider-crank mechanism. The previously developed levels of T_{CH} thus appeared to be the maximum practicable. Additional damping could be generated, if needed, through the use of a large dashpot in parallel with the actuating linkage. However, such a dashpot was not apparently needed, as was shown through investigation of the inherent damping of the rudder.

C. RUDDER

The description of the moments involved in the rotation of a rudder about its pivot, while moving through a fluid, would in general include functions involving the zero, first, and second-order derivatives of rudder angle with respect to time. That is, if a moment balance were written for a rotating rudder, the equation could in general take the following form:

$$M = f_1(\ddot{\theta}) + f_2(\dot{\theta}) + f_3(\theta) \tag{25}$$

where f_1, f_2, and f_3 would be functions of some yet-to-be-determined form. Further consideration of the natures of f_1 and f_3 revealed that expressions for these two functions were present in the baseline simulation. If $f_2 = f_3 = 0$, the general expression is reduced to

$$M = f_1(\ddot{\theta}) \tag{26}$$

and f_1 is recognized as being of the form

$$f_1 = I\ddot{\theta} \tag{27}$$

where I is the polar moment of inertia of the rudder and its fluid added mass. If $f_1=f_2=0$, f_3 is recognized as the sum of all θ - dependent parameters in the rudder, including the hydrodynamic torque caused by the rudder lift and the difference between the location of the rudder's pivot and its center of pressure, and the θ - dependent portion of the system friction.

The function $f_2(\dot{\theta})$ was assumed equal to zero in the baseline simulation; that is, no $\dot{\theta}$ - dependent effects were included in the rudder's equation of motion (Eqn. 8). The validity of this assumption was examined in the final portion of the investigation of load and linkage damping.

1. Existence of a Non-Zero Function $f_2(\dot{\theta})$

Initial considerations of the problem involved the search for any indication that a non-zero function $f_2(\dot{\theta})$ even existed. Intuitively, such a relation should exist in some magnitude, at least under a condition where the rudder was subjected to a constant turning rate while immersed in a stagnant, viscous fluid, since power would necessarily be expended to keep such a structure moving under these conditions, thus resulting in some level of torque being applied to the rudder shaft. This applied torque, then, would by Eqn. (25) be equal to $f_2(\dot{\theta})$, and therefore f_2 could not be identically zero.

Another indication of the existence of a non-zero f_2 was provided by Landweber [18], who indicated that forces on lifting surfaces in unsteady motion were due to a combination of inertia effects and circulation, and that a transient variation did exist in the circulation around a thin airfoil impulsively given an angle of attack α, causing a transient behavior

of the lift coefficient of such a surface. Additionally, Theodorsen [19] studied the forces on a foil undergoing harmonic oscillations in connection with studies of control surface flutter and aerodynamic instability, and found that the actual lift coefficient was related to a quasi-steady lift coefficient corresponding to the instantaneous angle of attack of the foil, and time. Thus, the existence of a non-zero function $f_2(\dot{\theta})$, while not confirmed by the above references, was at least shown to be plausible. The writer therefore attempted to locate any work that had been done in the analysis of the forces and turning moments on airfoils or rudders subjected to constant turning rate.

2. Damping in a Rudder Immersed in a Stationary Fluid

No references were found describing the resisting torque developed by a rudder subjected to a constant rate of rotation while immersed in a viscous fluid. Accordingly, the writer attempted to approximate the drag which could be expected, using elementary concepts and simplifying approximations.

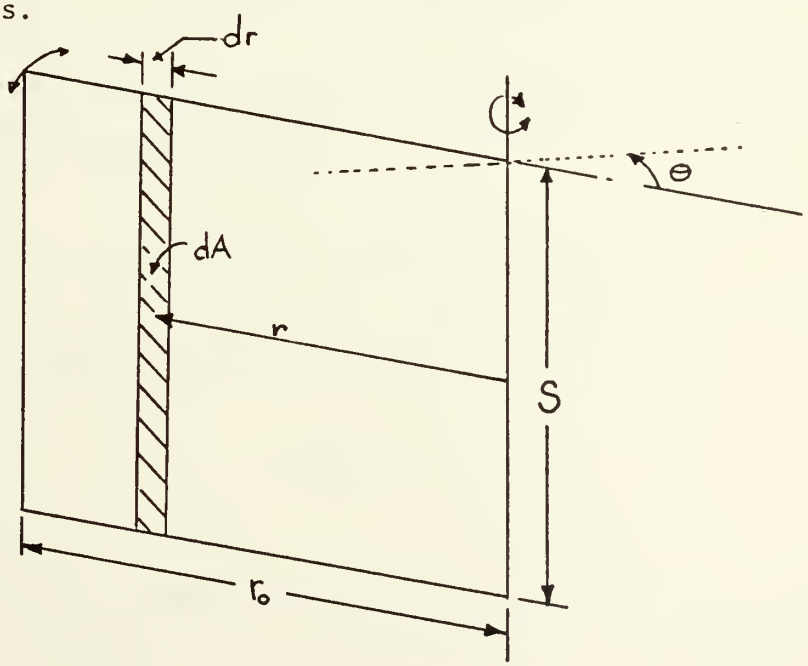

Figure 15. Rudder Construction Assumed For Stationary Rudder Torque Calculation

The rudder was approximated by a series of very small flat plates, assumed to be separated from each other so that the flow could move around the plates (Figure 15). For a flat plate placed in a stream flowing perpendicular to the plane of the plate, the drag force F_D can be expressed as

$$F_D = C_D \left(\frac{\rho V^2}{2} \right) A_p \tag{28}$$

where C_D in this case is the drag coefficient, ρ is the density, A_p is the area of the small plate, and the velocity V is related to the radius r and the angular rate of rotation $\dot{\theta}$ by $V = r\dot{\theta}$. Thus, for a differential area dA_p,

$$dF_D = C_d \left(\frac{\rho r^2 \dot{\theta}^2}{2} \right) dA_p$$

If the area is assumed to be equal to the span of the rudder S times the incremental distance dr, $dA_p = Sdr$, then

$$dF_D = C_D \left(\frac{\rho \dot{\theta}^2 r^2}{2} \right) Sdr$$

The incremental torque dT_R caused by F_D developed at a distance r from the pivot point of the rudder would be

$$dT_R = C_D \left(\frac{\rho \dot{\theta}^2}{2} \right) Sr^3 dr \tag{29}$$

Thus, for the portion of the plate from r = 0 to $r = r_o$,

$$T_R = \frac{C_D \rho S r_o^4}{8} \dot{\theta}^2 \ . \tag{30}$$

For a flat plate in a normal stream with a large S/dr ratio, C_D is approximately 1.95 [20]. For the two rudders of a typical submarine, the following physical parameters are representative:

Parameter	Value
S	10 Feet
r_o, rear portion	7 Feet
r_o, forward portion	3 Feet
ρ, sea water	64 lbm/ft^3

The entire $\dot{\theta}$ - dependent torque would be equal to the sum of the effects of both upper and lower rudders, including forward and aft portions:

$$T_{\dot{\theta}} = 2\ (T_{R_{FORWARD}} + T_{R_{AFT}})\ . \tag{31}$$

Substituting in the previously mentioned values, it is found that

$$T_{\dot{\theta}} = 88\ \dot{\theta}^2,\ \text{in.-lb}_f \tag{32}$$

when $\dot{\theta}$ is expressed in degrees per second. If $\dot{\theta}$ = 10 deg/sec, $T_{\dot{\theta}max}$ = 8800 in.-lbf. If an asymmetric square analog component and a potentiometer were placed in the simulator as in Figure 16, this source of damping could be modeled.

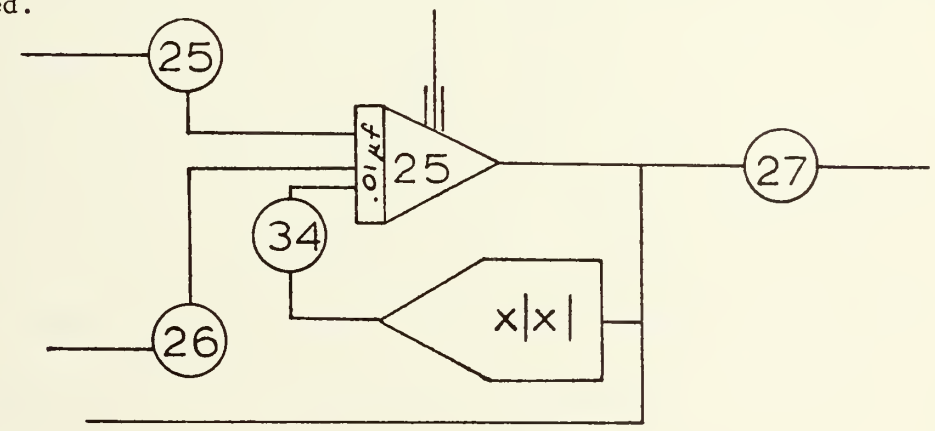

Figure 16. Analog Circuit Diagram for Introduction of $T_{\dot{\theta}}$

The appropriate potentiometer setting expression for simulating $T_{\dot{\theta}}$ would be

$$a_{34} = \frac{T_{\dot{\theta}_m}}{100\dot{\theta}_m I\beta}\ . \tag{33}$$

Substituting numerical values,

$$a_{34} = .968 \times 10^{-3}. \qquad (34)$$

Thus, the initial estimate of available rudder drag at zero velocity indicated negligible amounts of damping were present in the rudder turned at a constant rate in a stationary fluid. The writer felt that the results were inconclusive, however, since the assumptions which were made in the calculation of T_R were very rough indeed. The rudder was not formed of many small strips with spaces between them; nor was the flow as simple as that described by the model. Such a complicated flow as would be present along the surface of a large flat plate rotating in a quiescent fluid required much more analysis and study than the writer afforded it. He therefore concluded that future studies in this area were necessary, and set aside consideration of the stationary rudder case.

3. Damping in a Rudder Immersed in a Moving Stream

A literature search revealed that an analysis had been made of the torque behavior of a turning rudder immersed in a moving stream. Okada [21] published a paper dealing with the effect, which was subsequently expanded by Kennard and Leibowitz [22] in their studies of rudder performance as affected by ship turning, steady change of rudder angle, and propellor race.

Kennard and Leibowitz [23] noted that the twisting moment observed on a rudder shaft while the rudder is being turned may differ considerably from its value when the rudder is stationary. They went on to explain that this effect was due to circulatory motions around the foil caused by viscosity effects of the water, which subsequently generate vortex sheets in the water downstream from the rudder's trailing edge, and cause moment-modifying variations in the pressure distribution over the rudder's surface.

Variations from steady state twisting moments by as much as thirty percent were mentioned as being observed in rudders turning at constant rates.

The mathematical difficulties associated with the problem were simplified by several approximations. The rudder was replaced by the flat plate, shown in Figure 17, of uniform chord C and infinite vertical span. The water was assumed to approach the plate at a uniform rate and at an angle of attack α; its velocity was denoted by U. The rudder twisting moment per unit span was identified as M_H, and was assumed positive when operating in a direction to decrease α. The pivot point of the plate was identified as H, and was located at a distance hC from the leading edge, h being assigned some numerical value between 0.25 and 0.50. The rudder turning rate was assumed positive for increasing angles of α.

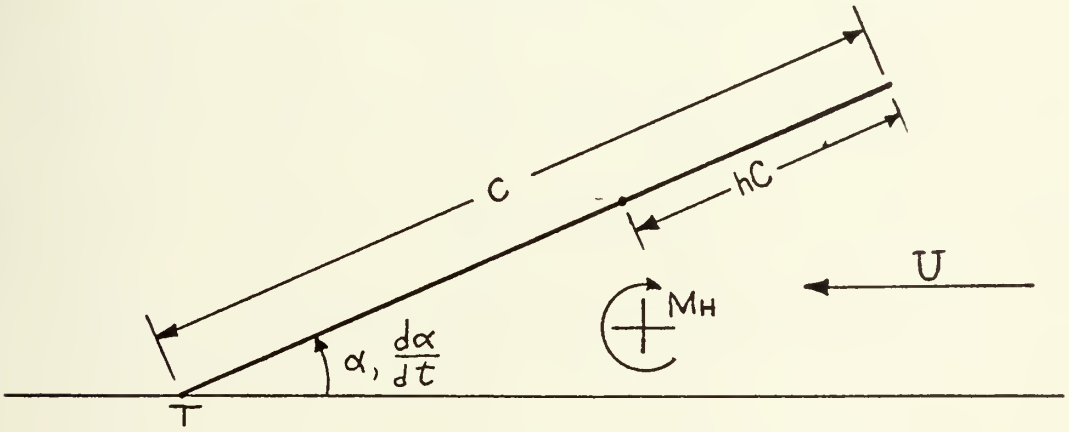

Figure 17. Flat Plate Approximation to a Rudder Turning at Constant Rate

M_H, the twisting moment per unit span, was placed in nondimensional form by dividing it by (1/2) C^2U^2, to form the dimensionless moment coefficient C_{MH}. An expression for C_{MH} was then derived, with C_{MH} being represented as the sum of a quasi-stationary part C_{MHO}, and a $\dot{\theta}$ - dependent part, ΔC_{MH}. Thus,

$$C_{MH} = C_{MHO} + \Delta C_{MH} \qquad (35)$$

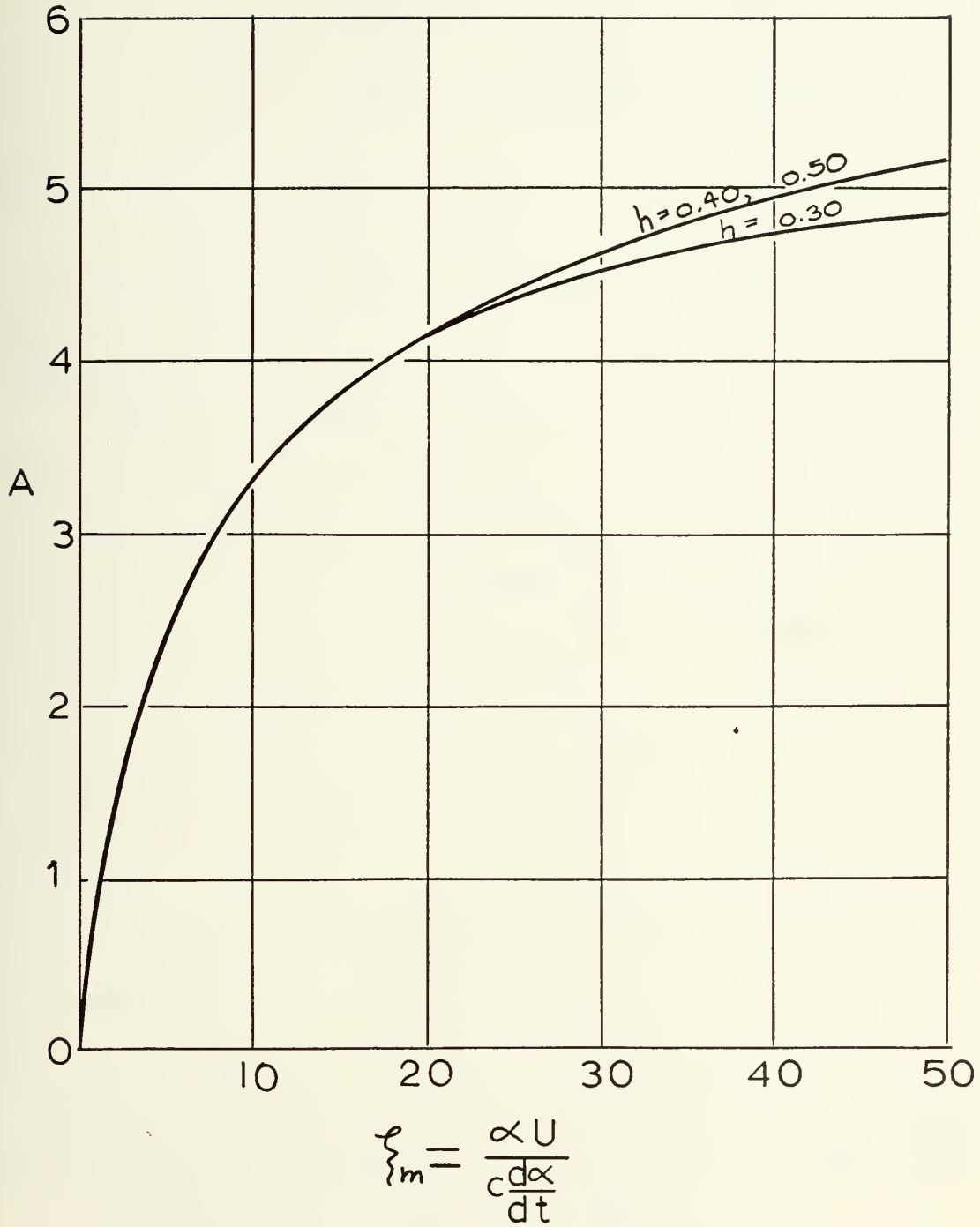

FIGURE 18

A VERSUS ξ_m

where

$$C_{MHO} = (\frac{1}{4} - h)\ 2\pi\alpha \tag{36}$$

$$\Delta C_{MH} = (\pi\Omega)\left[(\frac{3}{4} - h)(1-2h) - (\frac{1}{4} - h)A\right] \tag{37}$$

and

$$\Omega = \frac{C}{U}\frac{d\alpha}{dt}$$

and A is a function of Ω and α. The effect of A is to increase the value of ΔC_{MH} as α increases, as is shown in Figure 18.

Kennard and Leibowitz reported that the expression for C_{MHO} was not entirely correct, due to the neglect of a nonlinear effect in its development. That nonlinear effect concerns the aft movement of the center of pressure in a rudder as α is increased, which causes a change in the sign of C_{MHO} with increased α. Also, they indicated that values for ΔC_{MH} obtained from model tests suggested that the calculated values of ΔC_{MH} were somewhat too high, although the scatter of the experimental data in the tests was considerable. They further concluded that the general trends resulting from turning real rudders in water were modeled in their theory, although values for ΔC_{MH} were somewhat too high, such as a calculated increase in one case where h = 0.3 of roughly 40 percent, where in practice the increase due to ΔC_{MH} ranged from 15 to 40 percent. It was suggested that tests with larger rudders would be worthwhile, and that refinement of the analysis was needed, expecially in including the effects of finite rudder spans.

4. Application to the Simulation Problem

The analysis just described seemed to be applicable to the simulation problem. Although the expression for C_{MHO} was apparently unrealistic, the development of ΔC_{MH} was apparently useful in predicting the effect of rudder turning on the observed moments on a rudder, although calculated values

seemed to be somewhat higher than values which were experimentally obtained. In spite of its inherent shortcomings, incorporation of this modeling of the effect of rudder turning rate on the observed twisting moment seemed justified in light of the reported magnitudes of change in twisting moment observed in practice.

In order to apply the above analysis to the simulation, several assumptions were made. It was assumed that α was identical to θ ; that is, that the fluid flowed parallel to centerline of the submarine. Analysis of drawings of the SSN-671 submarine rudder revealed that h was approximately equal to 0.28; in order to compensate for the reported high nature of the calculated ΔC_{MH}, and to simplify calculations, h was assumed to be 1/4, thus eliminating dependence on A. Also, the sign convention of M_H was reversed to conform to the simulation's convention. The above assumptions when used in the expression for ΔC_{MH} resulted in

$$\Delta C_{MH} = -(\pi \frac{C}{V} \frac{d\theta}{dt})(\frac{1}{4}) \quad . \tag{38}$$

Re-dimensionalizing to form ΔM_H, the change in twisting moment per unit span due to $\dot{\theta}$, and then multiplying by the span length S, resulted in the expression

$$\Delta M_H S = -\frac{\pi}{8} \rho C^3 S V \dot{\theta} \quad . \tag{39}$$

For a SSN-671 rudder, the average value of C is about 10 feet, and S is also about 10 feet. In a typical submarine V can vary from zero to in excess of 35 ft/sec, and $\dot{\theta}$ was assumed in the baseline simulation to vary from zero to 10 degrees/sec. Assuming $\rho = 64$ lbm/ft^3, the maximum value of the twisting moment, $(\Delta M_H S)_{max}$ based on Vo = 35 ft/sec, would be

$$(\Delta M_H S)_{max} = 5.72 \times 10^5 \text{ in-lbf.} \tag{40}$$

Typically, a submarine has two rudders, of approximately the same design. The total twisting moment available would therefore be twice the above value, or 1.144×10^6 in-lbf. An expression for $\Delta M_H S/(\Delta M_H S)_{max}$ would be

$$\frac{\Delta M_H S}{(\Delta M_H S)_{max}} = -\left(\frac{V}{V_o}\right)\left(\frac{\dot{\theta}}{\dot{\theta}_{max}}\right) \tag{41}$$

$\Delta M_H S/(\Delta M_H S)_{max}$ is dependent only on $\dot{\theta}$ for a given value of V, and therefore could be simulated as damping across integrator 25 as in Figure 10. The appropriate expression for the potentiometer setting a_{33} would be

$$a_{33} = \frac{(\Delta M_H S)_{max}(V/V_o)}{I\dot{\theta}_{max}(100)\beta} \tag{42}$$

For $V = V_o$, and the conditions otherwise assumed above, since V appeared to be set equal to V_o for the other V - dependent parameters in the baseline simulation, $a_{33} = 0.1259$. A level of $0.12\frac{\dot{\theta}}{\dot{\theta}_m}$ feedback was previously found to be sufficient to approach a critically damped behavior of the simulation, and therefore eliminate the oscillations for the system. Apparently, then, a theoretical justification for the inclusion of that much damping in the system had been found. The fact that ΔC_{MH} was dependent on V did not allow the extension of the above damping levels to lower velocity, since as V decreases, so must the level of damping. Through communication with Mr. Johnson of the NSRDC, the author was led to believe that the damping effect somehow assumed a significantly large value even at low or zero velocities, thus indicating the existence of some unexamined or undiscovered contributing effects such as those previously discussed, which would be independent of V. More work in the area of rudder twisting moment and lift variance with rudder turning angle and other parameters obviously could be done.

5. Summary

The investigation of linkage and load damping resulted in the location of a significant source of $\dot{\theta}$ - damping in the motion of a rudder immersed in a moving fluid. A significant amount of damping was evidenced by the large variation of the observed twisting moment produced by the turning of a rudder from that which would be observed if the rudder were held stationary at a given angle of attack. On the basis of rudimentary analysis, no large amounts of viscous damping were located in the packings, or the crosshead structure, although a slight amount of damping could be caused in the crosshead through redesign of the structure. A very rough estimate of the twisting moment observed on a rudder immersed in a stationary fluid indicated that little available damping existed unless the rudder was being moved through the fluid. Obviously, more analytical and experimental research needs to be done concerning the transient lift and twisting moment characteristics of moving and stationary rudders in fluid flow fields.

IV. RECOMMENDATIONS FOR FURTHER WORK

Several topics were identified as requiring investigation during the progress of this project. Due to time limitations, the writer was unable to pursue any of them in detail. Subjects uncovered in the initial investigation which remained significant at the end of the period that this report covers included the need for examination of the actual performance of submarine steering control systems under varying conditions, including a wide range of ship velocities. Studies of the effect of using a higher order servovalve and uncompensated actuator models in the simulation are necessary. Possibly, the re-checking of the consistency of the numerical values used in the baseline simulation is warranted, although the discovery of a significant source of system damping seemed to make this unnecessary. Additionally, the investigation of linkage and load damping emphasized the need for continuing research into unsteady rudder system performance characteristics, including rudder lift and twisting moment variations with such variables as rudder turning rate, ship velocity, ship turning rate, hull configuration, and propeller race.

V. CONCLUSIONS

1. Analysis of unsteady rudder behavior identified a significant source of rate-dependent torque which had been neglected in the development of a submarine steering control system's analog simulation. Programming of representative levels of feedback in the simulator virtually eliminated oscillations in rudder rate and load pressure drop which were thought to be unrealistic.

2. The actual performance characteristics of a submarine steering control system under varying operational conditions appeared to be loosely defined, and quantitative studies of system performance seemed to be necessary in order to continue the development of a realistic simulator.

3. Studies showed that the inclusion of more complex models of the servovalve and actuator could have important effects on the flexibility and realism of the simulator, and that further work should be done to accomplish this end.

4. Continuing theoretical and experimental research in the field of rudder behavior under unsteady conditions was suggested in order to improve the current concepts employed in steering system design and simulation.

Appendix A

Explanation of Notation

1. Sat (x) $^{uL}_{LL}$

$$Sat(x)^{ul}_{ll} = \begin{cases} ul & x>ul \\ x & ll \leq x \leq ul \\ ll & x<ll \end{cases}$$

This can be represented graphically as follows:

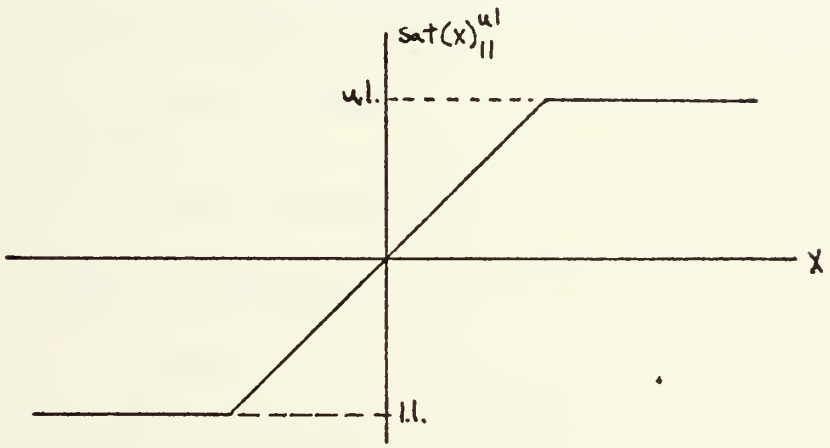

2. Sgn(x)

$$Sgn(x) = \begin{cases} +1 & x>0 \\ 0 & x=0 \\ -1 & x<0 \end{cases}$$

This can be represented as follows:

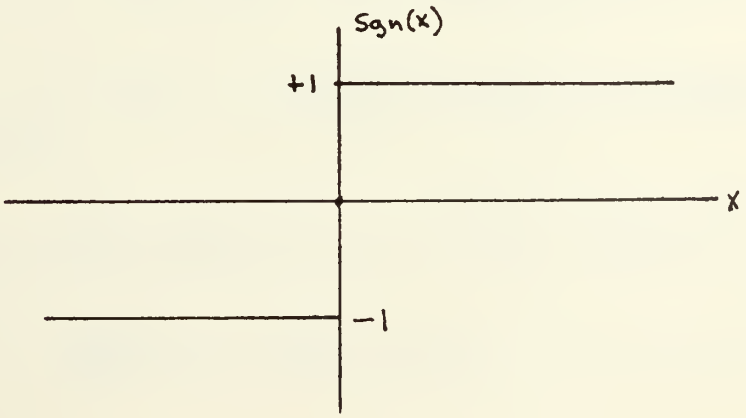

LIST OF REFERENCES

1. Morse, Allen C., Electrohydraulic Servomechanisms, p. 64, McGraw-Hill, 1963.

2. Morse, Allen C., Electrohydraulic Servomechanisms, p. 63, McGraw-Hill, 1963.

3. Merritt, H.E., Hydraulic Control Systems, p. 215, Wiley, 1967.

4. Johnson, G., NAVSHIPRANDCEN, Code 2762.3, Personal Communication.

5. Morse, Allen C., Electrohydraulic Servomechanisms, p. 142, McGraw-Hill, 1963.

6. Kendall, W.T., Code 260.41, Mare Island Naval Ship Yard, Vallejo, Ca. 94592, Personal Communication.

7. Johnson, Guy, Unclassified letter to R.H. Nunn describing the simulation, 20 December 1971.

8. Johnson, Guy, Telephone Communication, February 1972.

9. Smith, Leeland, Code 260.4, Mare Island Naval Ship Yard, Vallejo, Ca. 94952, Personal Communication.

10. Keller, G.R., Hydraulic System Analysis, pp. 139-142, Industrial, 1969.

11. Kendall, W.T., Code 260.41, Mare Island Naval Ship Yard, Vallejo, Ca. 94592, Personal Communication.

12. Chase, Leonard, Code 260.41, Mare Island Naval Ship Yard, Vallejo, Ca. 94592.

13. Merritt, H.E., Hydraulic Control Systems, p. 34, Wiley, 1967.

14. Merritt, H.E., Hydraulic Control Systems, p. 42, 43, Wiley, 1967.

15. Laughaar, H.L., Steady Flow in the Transition Length of a Straight Tube, Journal of Applied Mechanics, June 1942, A55-A58.

16. Krieth, F., Eisenstadt, R., Pressure Drop and Flow Characteristics of Short Capillary Tubes at Low Reynolds Numbers, ASME Transactions, July 1957 1070-1078.

17. Shapiro, H., Siegel, and Kline, J., Friction Factor in the Laminar Entry Region of a Smooth Tube, Proc. 2nd U.S. Natl. Congress of Applied Mechanics, June 1954 733-741.

18. Streeter, V., Handbook of Fluid Dynamics, 1st Ed., pp 13-35, 13-36, McGraw-Hill, 1961.

19. Theodorson, T., General Theory of Aerodynamic Instability and the Mechanism of Flutter, NACA Technical Report No. 496, 1949.

20. Hughes, W., Brighton, J., Shaum's Outline of Theory and Problems of Fluid Dynamics, p. 85.

21. Okada, S., Investigation of the Effect of the Angular Velocity of Steering Upon the Performance of Rudders, Technical Research Laboratory, HITACHI Shipbuilding and Engineering Company, Ltd., 1958.

22. Kennard, E., Leibowitz, R., Theory of Forces and Moments on Rudders as Affected by Ship Turning, Steady Change of Rudder Angle, and Propellor Race, NSRDC Acoustics and Vibrations Laboratory Technical Note AVL-238-940, pp. 47-71, January 1969.

23. Kennard, E., Leibowitz, R., Theory of Forces and Moments on Rudders as Affected by Ship Turning, Steady Change of Rudder Angle, and Propellor Race, NSRDC Acoustics and Vibrations Laboratory Technical Note AVL-238-940, p. 47, January 1969.

INITIAL DISTRIBUTION LIST

		No. Copies
1.	Defense Documentation Center Cameron Station Alexandria, Virginia 22314	2
2.	Library, Code 0212 Naval Postgraduate School Monterey, California 93940	2
3.	Professor R.H. Nunn, Code 59 Nn Department of Mechanical Engineering Naval Postgraduate School Monterey, California 93940	2
4.	Ensign Ernest E. Wessman 4901 South 4135 West Kearns, Utah 84118	2

Security Classification

DOCUMENT CONTROL DATA - R & D

(Security classification of title, body of abstract and indexing annotation must be entered when the overall report is classified)

ORIGINATING ACTIVITY (Corporate author)	2a. REPORT SECURITY CLASSIFICATION
aval Postgraduate School onterey, California 93940	Unclassified
	2b. GROUP

REPORT TITLE

nalysis and Simulation of a Submarine Steering Control System

DESCRIPTIVE NOTES (Type of report and inclusive dates)

aster's Thesis; June 1972

AUTHOR(S) (First name, middle initial, last name)

rnest Everett Wessman

REPORT DATE	7a. TOTAL NO. OF PAGES	7b. NO. OF REFS
une 1972	76	23

CONTRACT OR GRANT NO.	9a. ORIGINATOR'S REPORT NUMBER(S)
PROJECT NO.	
	9b. OTHER REPORT NO(S) (Any other numbers that may be assigned this report)

DISTRIBUTION STATEMENT

Distribution limited to U. S. Government Agencies only; Proprietary information, 8 August 1972. Other requests for this document must be referred to Naval Postgraduate School, Monterey, California, 93940, Code 023.

SUPPLEMENTARY NOTES	12. SPONSORING MILITARY ACTIVITY
	Naval Postgraduate School Monterey, California 93940

ABSTRACT

An existing computer simulation of a hydraulic submarine steering control system was analyzed to determine the source of its unrealistic behavior, which included verifying mathematical equations and numerical parameters, duplicating the simulation on another computer, and investigating the validity of the assumptions made in its development. Rudder turning rate and load pressure drop oscillations which were thought to be unrealistic were caused by the neglect of significant rudder moments related to the control surface turning rate. Knowledge of actual system performance was found to be incomplete and further research was suggested. Potentially beneficial modifications in the servovalve and actuator simulators were identified. Continuing work in the field of unsteady rudder behavior was suggested in order to improve simulator and actual system designs.

DD FORM 1 NOV 65 1473 (PAGE 1)

S/N 0101-807-6811

Security Classification

A-31408

KEY WORDS	LINK A		LINK B		LINK C	
	ROLE	WT	ROLE	WT	ROLE	WT
ring						
lation						
aulic						
er						
arine						